Soft-linking of improved spatiotemporal capacity expansion model with a power flow analysis for increased integration of renewable energy sources into interconnected archipelago

Marko Mimica[*a], Dominik F. Dominković[b], Vedran Kirinčić[c], Goran Krajačić[a]

[a]Department of Energy, Power Engineering and Ecology, Faculty of Mechanical Engineering and Naval Architecture, University of Zagreb, Ivana Lučića 5, 10002 Zagreb, Croatia

[b]Department of Applied Mathematics and Computer Science, Technical University of Denmark, Matematiktorvet, 2800 Lyngby, Denmark

[c]University of Rijeka, Faculty of Engineering, Department of Electric Power Systems, Vukovarska 58, 51000 Rijeka, Croatia

email: mmimica@fsb.hr

Abstract

This present study offers a novel approach for the improvement of energy planning. This has become increasingly important as higher penetration of variable energy resources and increased interconnection between the different energy sectors require more detailed planning in terms of spatiotemporal modeling in comparison to the presently available approaches. In this study, we present a method that soft-linked the energy planning and power flow models, which enabled fast and reliable solving of optimization problems. A linear continuous optimization model was used for the energy system optimization and the non-linear problem for the power system analysis. The method is used to compare different energy planning scenarios; further, this also offers the possibility for implementation assessment of the proposed scenarios. The method was applied to interconnected islands for five different scenarios. It was determined that the detailed spatial approach resulted in 26.7% higher total system costs, 3.3 times lower battery capacity, and 14.9 MW higher renewable energy generation capacities installed than in the coarser spatial representation. Moreover, the results of the power flow model indicated that the highest voltage deviation was 16% higher than the nominal voltage level. This indicates the need for inclusion of implementation possibility assessments of energy planning scenarios.

Keywords: energy planning; soft-linking; Calliope modeling framework; power flow; renewable energy sources; energy system analysis

Nomenclature

Parameters	
i, j	Nodes in the power system
n	Total number of nodes in the power system
g	Total number of generating nodes in the power system
ϕ	The phase angle between current and voltage [rad]
$\overline{Y_{ij}}$	Phasor value of admittance between nodes i and j
Y_{ij}	The scalar value of admittance between nodes i and j [S]
θ_{ij}	The phase of the admittance between nodes i and j [rad]
Q_{min}, Q_{max}	Minimum and maximum values of reactive power [MVar]
ε	Accuracy of the iterative procedure
Variables	
$\overline{V_i}$	Phasor value of the voltage at node i
V_i	The scalar value of the voltage at node i [kV]
ΔV	Voltage deviation [kV]
δ_i	Voltage angle at node i [rad]
$\Delta\delta$	Voltage angle deviation [rad]
P_i	Active power at node i [MW]
ΔP	Active power deviation [MW]
Q_i	Reactive power at node i [MVar]
ΔQ	Reactive power deviation [MVar]
J_1, J_2, J_3, J_4	Elements of the Jacobian matrix
Additional nomenclature	
S1, S2, S3, S4, S5	Analyzed scenarios
X1, X2, X3, X4, X5, X6, X7, X8	Modeled locations in the case study

1. Introduction

1.1.Background

Although islands have brought about a negligible impact on the rising issue of climate change, they will be the first ones that will experience its negative consequences [1]. For these reasons, there are two important initiatives in the European Union (EU) in terms of discussing the climate changes on the islands. First is the "Smart Islands Initiative" [2], which represents a bottom-up approach for the development of the islands' communities. This document presented ten goals for maximizing islands' potential and transforming them into living labs for testing advanced solutions for the energy transition that can later be transferred to the mainland. Second is a top-down document from the EU Commission [3] that aims to achieve sustainable communities on islands with clean and low-cost energy production.

These efforts need to be matched with the increased accuracy of the energy planning processes developed by the scientific community, especially for systems with the high share of variable renewable energy sources (RES). Moreover, the implementation possibilities of the proposed energy planning scenarios in the power system need to be further researched. The introduction of variable RES often creates voltage difficulties in the power system grid [4]; the latter has been deemed essential as a distribution system operator will deny permits to projects that integrate a large amount of variable RES if grid code is violated. The method proposed in this study enables a finer modeling of the energy planning scenarios and their application possibilities assessment in the existing power system infrastructure.

1.2.Literature review

Energy planning methods for islands have been extensively researched throughout the years. The authors in [5] presented the case study of S. Vicente, Cape Verde, where they analyzed the possibility of creating an energy system based only on wind power and pumped hydro plant. This particular study was further examined in [6] where authors included the water system by considering the desalination plant. The study showed that the integration of these two sectors resulted with a 36% increase in the renewable generation. Likewise, Child et al. [7] presented several energy planning scenarios on an hourly basis for the Åland Islands, which have the similar grid topology as the Krk island, with the conclusion that it is possible to achieve a 100% renewable production. Curto et al. [8] proposed a renewable energy mix based on the monthly time resolution and without application implications of the proposed scenario for the Ustica island. Depending on the investment cost of a battery, the authors in [9] showed that it is possible to achieve renewable energy share from 35.1% to 58.8%, but the study did not show the detailed operation of such system. Evidence from the study in [10] showed that a 100% renewable island such as La Gomera is economically and technically feasible. The application of the finer energy planning approach would enable a more detailed overview of the flexibility technologies (e.g., batteries) operation in this study [10]. A comparative study [11] indicated that the renewable energy mix can satisfy 87% of annual electrical energy demand on Fiji and 46% on the Balearic Islands. Comparison analyses based on rough time and spatial resolution can also provide somewhat more information; however, the results would be more significant if a finer approach would be considered. These analyzed studies had several similar research gaps. Most of these studies [5-11] considered the rough time resolution (hourly resolution or higher); they did not consider spatial distribution nor did they propose an approach for the implementation possibilities of considered energy planning scenarios in the power system grid.

Thus, the approach presented in this study proposed solution for all three research gaps. Moreover, this paper analyzed four different sectors, which is a significant advancement in comparison with the studies [5-11] that focused only on one or two sectors.

The following studies have focused either on a fine temporal resolution or fine spatial resolution. Mixed-integer linear programming was expanded with receding horizon model predictive control (RH-MPC) in [12] for the integration of different energy vectors on a half-hourly temporal resolution. In the case study for the carbon-neutral Canary Islands [13], it was determined that it is possible to completely cover local electricity and heating and transport demands with just utilizing local resources. The importance of islands' interconnection and the demand response was presented in [14] where the share of the renewable generation reached 85% in the final energy consumption of the interconnected system. Flexibility options were extensively discussed in these studies [12-14] by applying the coarser time resolution. The approach presented in this study offers a significantly finer overview of the operation of the flexibility providers such as batteries.

Spatially distributed modeling is necessary for the modeling of advanced technologies that are being introduced in the energy system. For example, spatial distribution was considered in [15] where the authors observed prosumer behavior. The study [16] used the spatially distributed model for measurement of network energy efficiency exchange. The soft-linking approach between different models was applied in several studies in order to reduce the computational time of the simulations. For example, soft-linking between the unit commitment model and the multi-sectoral model was used in the [17], whereas the energy planning model was soft-linked with the transport behavioral model in [18]. The aforementioned studies [12-18] did not provide a comparative analysis that would analyze the benefits of more detailed spatial and time modeling. Moreover, the current state-of-the-art analysis revealed that none of the analyzed papers, which focus on high RES energy system planning, has provided detailed electrical power grid analysis. The approach proposed in this study enabled a detailed comparison that clearly illustrated the pros and cons of different modeling approaches, highlighting the importance of electric power grid analysis.

The authors in [19] conducted the analysis on a 5-minute temporal resolution; however, the application possibilities were not analyzed. Load flow is a commonly used method for power system state assessment [20] and can be used for the assessment of the application possibilities of the energy planning scenarios. Since load flow is a non-linear and non-convex problem, several algorithms such as Gauss-Seidel or, the more common, Newton-Raphson method are

used for solving them. Although novel methods based on neural networks such as in [21] have emerged, Newton-Raphson method has proved to be sufficient for the power grids with the low ratio between the resistance and the reactance. The study [22] used the power flow to assess the impact of different strategies for the sizing the energy communities with battery and photovoltaics, however no capacity expansion model was considered. This paper proposed a joint approach with coupling of capacity expansion model and the power flow method, which enables precise estimation of the application possibilities of the energy planning scenarios.

1.3.Contributions

The aforementioned studies indicate that most of the simulations of energy systems on the islands are conducted on hourly time resolution and mostly do not consider the geographical distribution of energy resources and demands. Analyzed studies focus either on higher temporal or spatial distribution, but they do not consider them jointly. Analyzed studies failed to examine the technical changes in the power system steady state, which makes it hard to assess whether the proposed scenarios can be implemented in the electric power system or not. To the best of our knowledge, this is the first study that has analyzed island energy systems with high spatial and temporal resolution and with coupling of four sectors and has modeled and performed analysis of the power system on islands. This present study offers a solution to the gaps observed in current studies, thus representing a comprehensive approach in examining energy systems as summarized below:

- A detailed spatial coupled with a half-hourly temporal resolution analysis was performed by applying an electrical capacity expansion model
- Results obtained from the application of the energy system model were validated by conducting a power system analysis that provided insights about the energy system voltage and power flows
- The power transmission and distribution systems were modeled, thus enabling the checking of the power flows along the grid

To allow other researchers to repeat calculations and achieve the same results or improve them, the study also follows Open Energy Modelling Initiative for open energy modeling, with the entire model and code available at GitHub (link is provided in the acknowledgments).

This paper is organized as follows: the introduction and literature review are followed by the materials and methods section. The third section describes the case study; the results and

discussion are provided in the fourth section; and, in the fifth section, conclusions of this study are provided. The general overview of the presented approach is given in Figure 1.

2. Methods

2.1.Energy planning model

The Calliope modeling framework was used to develop the energy planning model. Calliope is a multi-scale energy systems modeling framework [23]. It is a free and open-source tool, which makes it easily accessible to everyone. The latter is in line with the push-in academia for radical transparency of the model assumptions, as well of the model implementation itself [24]. All of the code, as well as its documentation, are freely available online. The Calliope modeling tool is very versatile as it allows the modeler to create models with the user-defined temporal and spatial resolution as well as pre-model any technology that is relevant for the chosen case study. Hence, it is possible to use the tool for creating models at different scales, from urban districts to entire continents. The modeling tool was used, among others, for case studies of Bangalore, Cambridge, South Africa, and the United Kingdom [25].

The Calliope model used in this study was a linear continuous optimization model. The created model was a capacity expansion one, which included optimizing the operation of the system, as well as optimizing the capacities technologies to be installed. Its objective function was to minimize the total socio-economic costs throughout the target year. In the specific model developed in this paper, the objective function included annualized investment costs, fixed and variable operating and maintenance costs, as well as fuel and CO_2 costs. CO_2 costs were internalized in the form of CO_2 tax for the transport fuels, while a more complicated calculation was used for the import of electricity from outside of the system boundaries. To account for the CO_2 cost, it was taken into consideration that the EU Emissions Trading System (ETS) price was already included in the price of electricity that was settled on a day-ahead market in the reference year (e.g., the year 2017). To take into account a higher ETS cost in the target year (e.g., the year 2030), a difference between the projected ETS cost in the target year and the achieved ETS price in the reference year was added to the electricity cost in a form of the fixed carbon tax.

Constraints of the model were set to meet the half-hourly heating demand, cooling demand, electricity, as well as transport demand in each of the location. Satisfying the heating, cooling,

and electricity demands in each of the time-steps can be done by a wide range of technologies and storage solutions that are partly specific for a certain case study. The predefined technologies for the case study used in this paper are discussed in detail in the Case Study section. Meeting the transport demand could be done by gasoline, electric, and/or hydrogen vehicles. It was taken into account that for the same vehicle type, electric vehicles are 3.5 times more efficient compared to the gasoline vehicles and two times more efficient than the hydrogen vehicles, expressed as energy consumed per kilometer traveled [26]. The transport demand for electric and hydrogen vehicles was defined as the energy demand for charging/fueling of vehicles at specific time-steps, while for gasoline vehicles, it was considered that they can be fueled at any point of time without any capacity constraint. The electricity demand for transport was modeled as on-demand charge, while smart charging and vehicle-to-grid options were not modeled.

Furthermore, several factors in relation to location as well as scenario were imposed, as described in the Case Study section in more details.

The full mathematical model of the Calliope modeling framework can be read directly in [27]. The stated reference presents detailed documentation with well-explained system equations, as well as their implementation. The Calliope version 0.6.4 was used for the modeling presented in this paper.

Socio-economic costs were optimized in this paper. The socio-economic costs have been considered as a good representation of the costs of an energy system that are imposed on society. As opposed to the business-economic costs, they do not include different taxes and subsidies, as those are considered to be only internal redistributions within the society [28]. However, the costs of CO_2 were taken into calculation, as the CO_2 costs present internalization of the negative externalities that are imposed on the society through climate change.

The socio-economic analysis was further enhanced with the job-potential analysis of different technologies, in order to assess the impact of the energy transition on the local economy and community. This is an important segment necessary for the successful implementation of energy projects, which are often perceived negatively within the local community. Therefore, this study also calculated the job-years and permanent jobs created, as a result of proposed energy planning scenarios. The report [29] stated that the 1 MW of onshore wind power installed has resulted in 8.6 job-years and 1 MW of photovoltaic plants (PV) in 17.9 job-years related to maintenance, production, and installation of these technologies. Moreover, additional

0.2 and 0.3 local permanent jobs per MW of installed PV and onshore wind respectively will be created in relation to the maintenance of these installed plants. The same job creation potential was used in this study. However, it is also important to note that this study elaborates on the impact on the local and global economy. Only O&M jobs contribute to the local economy, while other jobs are related to the production and the development of the technology and contribute on the global scale. The obtained results were also put in the perspective of the local community where the proposed scenarios were located.

2.2.Power system analysis

High penetration of variable RES in the system often creates voltage problems in the grid, which can limit the potential capacity of variable RES that can be integrated to the grid, especially in the distribution grid [4]. Thus, to validate the results of the capacity expansion energy planning model, a more detailed transmission and distribution grid analysis was carried out in NEPLAN [30]. The method has included the modeling of 20 kV and 110 kV grid and included lines, transformers, nodes, loads, variable RES installations, and replacement model for the external grid. The data needed to model the power system is provided in Table 1. The required data include electrical parameters for lines, transformers, generation, and loads. Additionally, it is necessary to define the node type that can be one of the following:

- Referent node (slack or swing node)—the node for which voltage and voltage angle values are known
- Generation nodes (“PV” nodes)—the nodes for which the active power and voltage are known (these nodes have the regulation possibility)
- Load nodes (“PQ” nodes)—the nodes for which active and reactive power is known

To model the rest of the grid that is connected to the observed grid, the active grid model was defined with its electrical parameters.

Table 1. Necessary data for the load flow calculation

An element of the power system	**Required data for modeling**
Nodes	Nominal voltage; type of node (slack, generator, node)
Lines	Direct resistance; direct reactance; direct capacitance; length; current
Transformers	Nominal power; short circuit voltage; vector group; primary and secondary voltage ratio; losses; tap regulation
Active grid	Short circuit; short circuit three-phase apparent power; direct resistance and reactance ratio
Loads	Active power, cos(ϕ)
Renewable generators	Connection voltage; active power; reactive power; cos(ϕ); regulation (PQ for renewables)

Moreover, power flow was performed to obtain all-electric power grid vectors. In addition to active power, power flow also considers reactive power flows in order to represent the exact model. As power flow is a non-linear and non-convex problem, a Newton-Raphson algorithm (described in Appendix A) was used to obtain its solutions. Grid modeling and power flow analysis were necessary to validate energy planning scenarios, as well as to assess whether it is possible to implement developed energy planning scenarios. If the latter is not the case, the analysis will indicate where are the problems in the grid that need to be resolved. In case of unfavorable conditions in the power system grid, another solution could be to change constraints of the energy system model and obtain different results that could then be validated in the power system analysis.

2.3. The soft-linking approach and the overview of the method

The definition of soft-linking in this paper is as follows: soft-linking combines the output of one model as an input to the second model. By using the term "soft", we denote that the models are not run in parallel, but one after another. In this way, we do not increase the complexity of the models, as would be the case when hard-linking the two models. Hard-linking would combine both models together and result in one very complex model [31]. The reason for the application of the soft-linking approach is that running both models simultaneously would present a complex computational problem, especially because the power flow model is non-linear and non-convex. Thus, outputs from the energy planning model (installed capacity and energy production) are used in the power flow model in order to assess the implementation possibilities of the proposed scenarios. A soft-linked model can implement a feedback loop

between them if needed. For the case of this paper, this feedback loop was not needed and thus, it was not implemented.

The proposed method does not prescribe any specific procedure for the data collection. The input data for the model should be collected according to the available data sources. This proposed model offers a wide range of possibilities for the inclusion of different energy sectors, the definition of various technical parameters, and the definition of the arbitrary topology of the model. The proposition of a specific data collection method would limit the possibilities of the model; thus, this study aims to avoid such scenario. The Case Study section of this paper offers an example of what data can be used for the model.

The methods used in this paper can be summarized in eight steps. These steps included the creation of a specific integrated energy model for the selected case study, the usage of detailed temporal and spatial resolution, the linkage of the output of the energy planning model to the input of the power flow analysis, and the analysis of the results. The steps of the proposed method are stated below and the proposed soft-linking method is presented in Figure 1.

Step 1: Data inventory: Collect, check, and organize the data input for the model

Step 2: Topology of the analyzed Case Study: Definition of the locations and connections of the analyzed energy system as well as the types of technologies at each location following available spatial plans and data

Step 3: Energy system optimization procedure: Run the optimization model, extract results, and identify energy conversion and energy storage technologies to be installed, their combination, and capacity for every single node of the system

Step 4: Socio-economic analysis: Analyze the impacts of the obtained results on the local economy and society

Step 5: Soft-linking between the energy optimization model and the power flow model: Transform and prepare the output results from energy planning results into input data for the power flow model

Step 6: Define the power system grid parameters: Nodes, lines, transformers, generators, loads, and active grid

Step 7: Load flow analysis procedure: Solve non-linear equations using iteration methods and obtain voltage vector and power flows

Step 8: Results analysis: Installed capacities and operation of all technologies, impact on the power system grid, implementation possibilities of the proposed energy planning scenarios

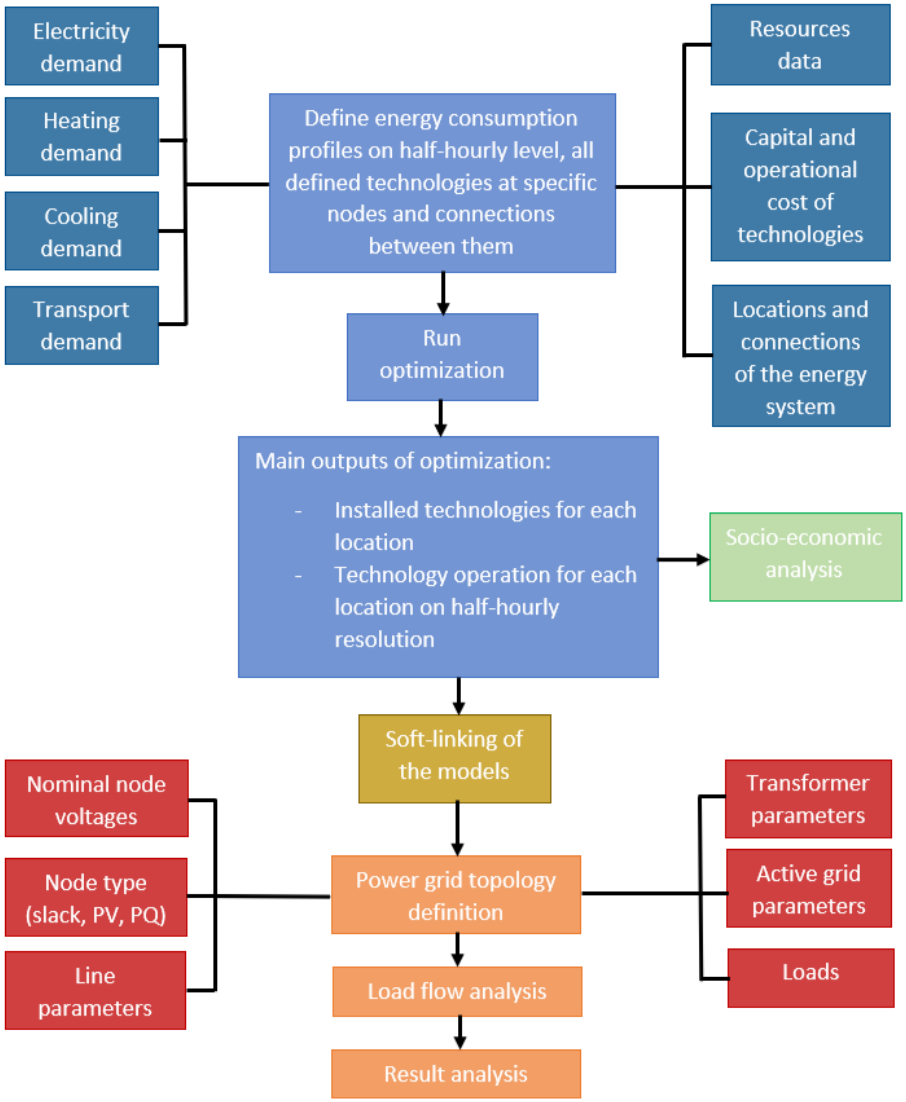

Figure 1. Presented energy planning framework. The data from the Calliope modeling framework that was used as inputs to the load flow model were as follows: the installation power of utility and residential generating technologies, electrified transport demand, and electricity demand for all locations.

3. Case Study

3.1.Geographical location

To test the proposed approach, a case study was conducted on the islands of the Kvarner archipelago, located in the north-west part of Croatia. The places are the island of Krk, Lošinj, Cres, Rab, Unije, Ilovik, and Sušak. Their location is part of the Mediterranean climate characteristic for Italy, France, Greece, and Spain. The total population of all islands has been determined to be 42 503 [32]. Krk is the largest island in Kvarner archipelago, with a population of 19 374 residents and is divided into three parts—the cities of Krk, Dunat, and Omišalj.

A half-hourly temporal resolution was used, and the model was run consecutively, meaning that no slicing and/or decomposition was applied. This approach allowed a detailed representation of the behavior of different storage types during different time scales, such as diurnal, weekly, monthly, and seasonal [33]. A proper spatial resolution was defined following the assessment of the current power grid and the population centers within the island. In total, eight different geographical locations were modeled. Three different locations were considered on the island of Krk (X1, X2, and X3), while two locations were considered for the nearby remote islands wherein their electricity demand need to be met through the island of Krk (X4 and X5). Furthermore, two locations were considered for the import/export interconnectors to the national (mainland) electricity grid (X6 and X7), whereas one location was considered for the potential wind offshore wind turbine (X8).

Two substations 110/20 kV are located in the cities of Krk (X1) and Dunat (X2) that are supplying electric energy to all islands of Kvarner archipelago. Substations in the cities of Krk and Dunat, as well as cities of Krk and Omišalj (X3), are connected with 110 kV line. The connection between Krk and mainland consists two underwater cables, one connecting Omišalj and Melina (X6) with a maximum capacity of 100 MW and another connecting the substation in city of Krk directly to Crikvenica (X7) on the mainland with a total capacity of 70 MW. Islands of Lošinj, Cres, Unije, Ilovik, and Sušak were considered as one location Lošinj (X4), while the island of Rab (X5) was considered as one location. Rab (X5) is connected to Dunat (X2) and Lošinj (X4) to Krk (X1), both with a 100 MW transmission line. All transmission capacities were fixed since there is no indication that they should be changed in the future. Additionally, potential offshore wind turbine plant (X8) near Omišalj was considered. The list

of the considered locations is provided in Table 2, while Figure 2 visually presents the locations of the case study with all connections between different locations [34]:

Table 2. List of the geographical locations, energy function, and reciprocal connections as designed in the Calliope model

Location	Name	Type	Connection to	Distributed generation
X1	City of Krk	Demand	X2; X3; X4; X7	Yes
X2	Dunat	Demand	X1; X5	Yes
X3	Omišalj	Demand	X1; X6; X8	Yes
X4	Lošinj	Demand	X1	No
X5	Rab	Demand	X2	No
X6	Melina	Import/export	X3	No
X7	Crikvenica	Import/export	X1	No
X8	Offshore wind turbine	Generation	X3	No

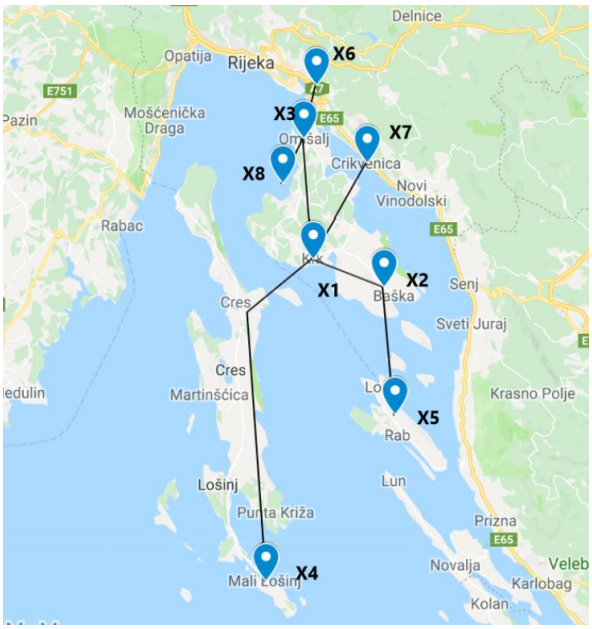

Figure 2. Geographic map showing nodes and their connecting network considered in the energy system modeling

3.2.Considered technologies and energy system related data

Different technology options were considered in this model. The following electricity technologies were included in this model: wind onshore, wind offshore, PV residential, utility-

scale PV, biogas engines (and gasification plants), a waste incineration plant, concentrated solar power, hydrogen electrolyzers and fuel cells (proton-exchange membrane technology), and a biomass power plant. In the heating and cooling sectors, the following technologies were considered: air-to-water heat pumps, ground-source heat pumps, electric boilers, biomass boilers, and solar thermal coupled with storage. Moreover, the following storage solutions were defined: Li-ion batteries, hydrogen storage, and heat accumulators for individual use. Finally, the transport sector included the following options: gasoline, electric, and hydrogen vehicles. The use of electric and hydrogen vehicles was modeled as energy storage satisfying the transport demand. A diverse range of technologies modeled for this case study included all the technologies that are suitable for distributed energy generation. Although there is a liquefied natural gas terminal under construction that will be connected to the gas grid and exported to the mainland, gas-fueled boilers and cogeneration plants were not modeled because of the EU bans on this carrier for household heating (e.g. [35], [36]). Nuclear power plants were not predefined, as their usually large capacities were considered as significantly too large for the collection of islands of the population and size considered in this case study.

Distributed generation was modeled on locations X1, X2, and X3. There have already been plans for the development of PV plants on the islands surrounding Krk; however, they are not considered because the development of these projects still needs to take place. Required input data were obtained from detailed measurements and reports that are available. Annual data for electricity, heating, cooling, transport, solar irradiation, and wind speed are provided in Table 3. All the data inputs are referred for the year 2017. The annual time course of energy demands and imports, as well as energy generation and export, was arranged with respect to the different energy sectors and referring to the entire energy system of Krk Island. The wind generation normalized pattern and the half-hourly cooling and heating curves were created using the data acquired from [37]. Moreover, the hourly PV generation pattern was acquired from the PV GIS database for different locations and interpolated to achieve half-hourly time resolution [38]. Thanks to the availability of detailed data on permanent and temporary occupied housings in Krk in [32], it was possible to estimate upper capacities for individual boilers and residential PVs. Half-hourly data of all the locations are openly available on the GitHub website, together with the applied model [39].

Table 3. Summarized input data for the case study. Full dataset available at [39]

Demand type	**Location**	**Demand quantity**	**Maximum load [MW]**	**References**
Electricity	X1	49 GWh	17	[40], [41], [42], [43]
	X2	68 GWh	20	
	X3	19 GWh	6	
Heating	X1	40 GWh	20.8	[40], [41], [42]
	X2	22 GWh	11.2	
	X3	11 GWh	5.8	
Cooling	X1	6 GWh	13.4	[40], [41], [42]
	X2	3 GWh	7.2	
	X3	2 GWh	3.8	
Transport	X1	12 GWh*	4.7	[44]
	X2	12 GWh*	4.9	
	X3	5 GWh*	1.5	
Resources	**Location**	**Capacity factor**	**Max capacity factor**	**References**
Solar	X1	0.162	0.9	[45]
	X2	0.15	0.88	
	X3	0.154	0.88	
Onshore wind	X1, X2, X3	0.254	1.0	[46]
Offshore wind	X8	0.35	1.0	[46]

** Transport equivalent electricity demand. If all the demand was to be covered by gasoline vehicles, the value would be 3.5 times higher, e.g., 42 GWh of gasoline for X1 location. If all the demand was to be covered by hydrogen, the resulting demand would be two times higher, e.g., 24 GWh for X1. This assumption allowed a resulting transport demand to be met by a mix of all three technologies.*

Table 4 presents the investment and O&M costs, as well as the main technical parameters for the modeled technologies. It is assumed that the prices reflect the 2030 technology prices. The interest rate applied in the model was assumed to equal to 10%, except for residential PV, which had a discount rate of 5%. The fixed O&M costs are dependable on the installed capacity, but this cost is the same for each year of the operation.

Table 4. Investment, technical, and O&M parameters of technologies considered by the model. The full list of parameters and technical constraints can be seen in [39]

Technology	**Investment cost**	**O&M fixed cost [€/kW]**	**O&M variable cost [€/MWh]**	**Efficiency**	**Lifetime [years]**	**Ref.**
Fuel cell (PEM)	1900 €/kW	95	-	50%	10	[47]
Electrolyzer (PEM)	1896 €/kW	163	-	58%	15	[47]
Hydrogen storage	11 €/kW	-	-	95%	25	[47]
Residential PV	1070 €/kW	12.8	-	100%**	30	[48]
Utility-scale PV	620 €/kW	8.1	-	100%**	35	[48]
Onshore wind	1120 €/kW	14	-	100%**	27	[48]
Offshore wind	2130 €/kW	40	-	100%**	27	[48]
CSP	2295 €/kW	-	2	100%**	25	[49]
Battery	143 €/kWh	-	-	95%	25	[47]
Heat accumulator	0.55 €/kWh	-	-	90%	25	[47]
Biogas Gasification	1810 €/kW	198		100%**	25	[50]
Biogas engine	950 €/kW	9.75		45%	25	[48]
Waste incinerator	10 500 €/kW	96	5.8	23.5% el	25	[48]
Biomass PP	6000 €/kW	288.9	7.8	29%	25	[48]
BIOboiler	680 €/kW	-	13.88	80%	20	[51]
Air source heat pump	1750 €/kW	-	0.5	COP 3.5 heating; 2.5 cooling	18	[51]
Ground-source heat pump	2750 €/kW		0.5	COP 5.5 heating; 3.5 cooling	20	[51]
Electric boiler individual	1000 €/kW	-	0.1	95%	20	[52]
Solar thermal individual	857 €/kW	16.2		100%**	25	[48]
Electricity grid*	0.01 €/kW/meter	-	-	96%	25	[53]

** Wind offshore site does not have a connection to the island grid; thus, if deemed optimal, this link needed to be built on top of the offshore wind turbine.*

*** Assumed 100% because the costs are related to the output power of those sources*

3.3.Considered scenarios

Three scenarios were modeled; further, two were included in the sensitivity analysis. The electricity prices for all the scenarios were taken for the year 2017 from CROPEX, a Croatian day-ahead power market [54], with the assumption that the same level of electricity prices can be expected for the period relevant for this study (the year 2030), except the expected cost increase of CO_2. The average ETS price of allowances in 2017 was 5.8 €/ton of CO_2 [55], while the projected ETS price in 2030 is 55 €/ton of CO_2, according to [56]. Thus, to account for the difference in the ETS price that was considered in the price of electricity in 2017 and the expected price in 2030, an additional carbon tax of 49.2 €/ton of CO_2 was added to the system. The carbon emission intensity of the Croatian mainland electricity was 250 kgCO2/MWh. Only the annual average carbon intensity of electricity was available; thus, the same carbon intensity was assumed in all the time-steps of the modeled year. Furthermore, none of the scenarios included any form of subsidies, as socio-economic costs were modeled in this case study.

The first scenario considered all the energy technologies without constraints. The second scenario allowed the electrification of transport by at least 25%, while the third by at least 65%. The third scenario also envisaged a minimum 5% hydrogen share in the transport sector, which was utilized for heavy transport modes. The share of the directly electrified transport sector (65%) was taken based on [44], which has shown that 72% of the transport sector could be directly electrified with the currently known technologies. The third scenario was also the basis for the two sensitivity analysis scenarios, in which the impact of the coarser temporal and spatial resolutions was considered.

To directly assess the differences between the detailed spatial and temporal resolution, a sensitivity analysis was performed by comparing the scenario with the highest share of renewable energy generation with completely the same case study (the same energy system) but using a coarser time resolution, as well as a coarser spatial resolution. The sensitivity analysis was run separately for the case of coarser time resolution from the case of the coarser spatial resolution. These analyses allowed for explicit comparison of the impact of time resolution and the spatial resolution on the capacity expansion modeling problems.

Export of electricity generated on the island was allowed in all the scenarios, and the income for those exports was determined to be equal to the matching hourly CROPEX price. Hence, the income from exporting electricity could lower the total socio-economic costs of the system. Scenarios are summarized in Table 5. However, it is important to note that islands remained

connected to the mainland in all the scenarios and that grid provided ancillary support to islands when needed.

Table 5. Scenarios applied to the model

Scenario	Transport constraint	Temporal resolution
S1	No constraint	Detailed spatial and half-hourly modelling
S2	A minimum 25% of electrified transport	Detailed spatial and half-hourly modelling
S3	A minimum 65% of electrified transport and minimum of 5% hydrogen for transport	Detailed spatial and half-hourly modelling
S4	A minimum 65% of electrified transport and minimum of 5% hydrogen for transport	Detailed spatial and hourly modelling
S5	A minimum 65% of electrified transport and minimum of 5% hydrogen for transport	Single geographic location and half-hourly modelling

S1 was chosen as a reference scenario. Meanwhile, S2 and S3 were chosen to explore the impacts of the introduction of different shares of different transportation types. Thereafter, S4 and S5 were compared to S3 and were chosen to demonstrate the improvements related to a finer resolution in time (S4) and space (S5). Indeed, S4 considered a coarser time resolution of 1 hour, while S5 applied just a single node to the simulated energy system.

3.4.Electric power grid analysis and solution algorithm

Power grid analysis was carried out for the highest RES penetration, as this should be considered the most challenging condition in keeping the voltage within the allowed limits. Two sub-scenarios were considered for this case as well: the first one, in which only distributed energy resources are considered without utility-scale production; and the second one, which includes utility-scale production connected to high voltage buses at substations Krk and Dunat. The analysis was conducted for two cases, i.e., minimum and maximum load, as is usually the case in grid connection projects [57]. It is considered that all loads work with $\cos(\varphi) = 0.95$ in order to include reactive power flow effects as well. The slack node is chosen to be Melina 400/220/110 kV substation (X6) because it has the highest regulation possibilities in the observed area. The measured voltage was obtained from the distribution system operator and it was equal to 115.5 kV for the maximum load and 121.22 kV for the minimum load. The

inclusion of the slack bus voltage data assured that the model is equivalent to a currently existing state.

The largest optimization problem was Scenario 3, and the following parameters have been determined to be associated with that scenario run. The model was run using the CPLEX optimization solver, using on average 4 cores. The average RAM utilization was 21 GB, while the max RAM use was 27.5 GB. The total run time was 1h 24 min, the optimization problem consisted of 6.92 million variables, and there were 1.12 million objective non-zeros.

4. Results

4.1.Installed technologies for S1, S2, and S3

As per the results of the case studies, it was determined that there is a high possibility for the integration of RES on the Krk island by 2030. The results were obtained for electricity, heating, cooling, and transport system for all analyzed scenarios. Figure 3 presents the power of installed technologies for electricity and thermal production. It can be observed that an increased share of electrified transport has led to higher installed capacities of renewable electricity generation. Moreover, the increased share of electrified transport without smart charging resulted in an increased power requirement of the battery storage system.

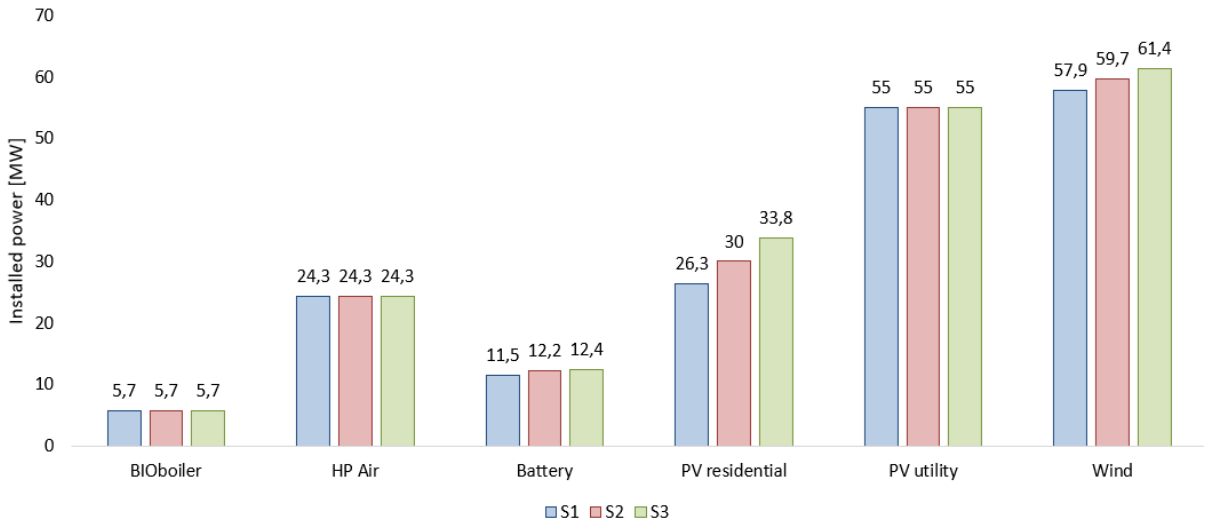

Figure 3. Installed power of electricity, thermal, and battery storage technology

Figure 4 presents the installed electricity generation capacities for all locations on the Krk Island for the S1, S2, and S3. Increase in the electrification of transportation has resulted in an increase

of 1.7 MW wind on the location X3 and an increase of 3.8 MW of residential PV on the location X2 in comparison with S2.

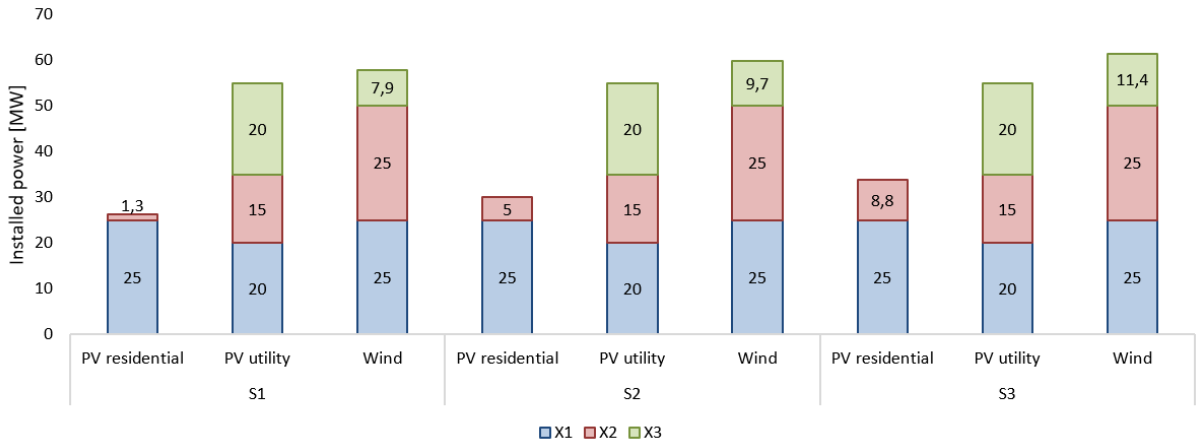

Figure 4. Distribution of installed electricity generation capacities for three scenarios

Different storage technologies and their capacities for the three modeled locations on the Krk Island are presented in Figure 5. In line with the previous results, the increase on electrified transport has also lead to the increase in the required battery capacity. The difference is visible in S2 where the battery capacity increased for 0.6 MWh, 0.7 MWh, and 0.1 MWh for three locations X1, X2, and X3, respectively, in comparison to the S1. Introduction of hydrogen in the transportation sector resulted in the requirements for hydrogen storage for S3. The hydrogen storage requirements were also present for different locations, namely, 1.4 MWh for X1 location and 5.2 MWh for X3 location.

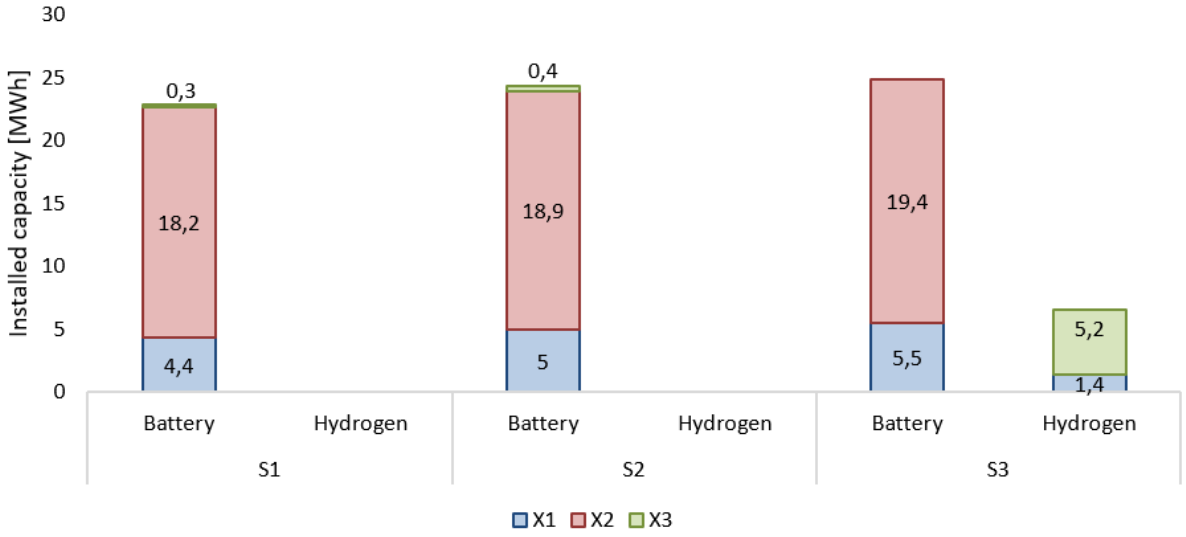

Figure 5. Storage capacity by considered technologies with reference to the Krk island locations and the three compared modeling scenarios. Heat accumulator value remained the same for all three scenarios (150 MWh)

The share of a particular transport type is presented in Table 6. The results showed that the minimum share of certain transport type constraints was activated in the optimization. Thus, the transport shares of different technologies were a result of the constraints of each particular scenario. Contrary to on-demand charging approach used in this paper, modeling smart charging or vehicle-to-grid could change the optimal mix of the transport sector [58]. However, this was left outside of the scope of this paper.

Table 6. Share of transportation type for S1, S2, and S3

Scenario	**S1**			**S2**			**S3**		
Transport type	EVs	Gasoline vehicles	Hydrogen vehicles	EVs	Gasoline vehicles	Hydrogen vehicles	EVs	Gasoline vehicles	Hydrogen vehicles
Share [%]	2	98	0	25	75	0	65	30	5

4.2.Sensitivity analysis between the S3, S4, and S5

As per the results of the sensitivity analysis, the approach used in this study showed significant improvements. Figure 6 presents the installed capacities of different technologies for S3, S4, and S5 scenarios. The comparison between half-hourly and hourly scenarios (S3 and S4) revealed a slight difference in the installed capacities. For example, S4 resulted in 1.2% less

installed power of residential PV in comparison to the S3. Installed wind capacities increased from 61.4 MW for S3 to 62 MW for S4. The difference between the two scenarios can also be observed for the installed battery storage power, which differentiates by 2.3 MW for the two scenarios. Meanwhile, the comparison between the spatially dispersed approach (S3) and the aggregated approach (S5) showed significant differences. The results of the S5 suggested significantly lower amounts of installed electricity generation power than for the case of S3. In this sense, the installed wind power reduced by 7 MW, while the installed power for the residential PV decreased by 8.1 MW. These results represent a change of 11.3% in the installed wind capacity and 24.3% in the installed residential PV capacity for the S5 in comparison to the S3.

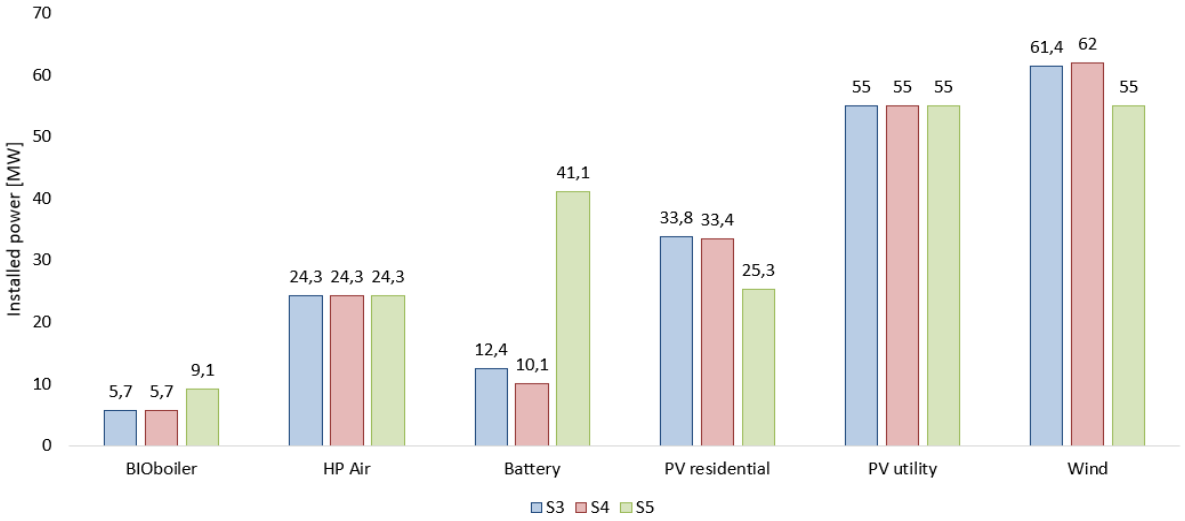

Figure 6. Installed capacities of different technologies for S3 and sensitivity scenarios

More detailed representation of the results for electricity generation technologies is provided in Figure 7. The results of S3, S4, and S5 for all Krk locations were compared. The difference between S3 and S4 was observed in the residential PV on location X2 (4.5% lower value for the S4) and the wind generation on the location X3 (5.3% higher value for the S4). The difference between S3 and S5 is more visible as the results of S5 indicated lower capacities of the installed technologies. Moreover, spatially distributed scenario contained a significantly larger amount of information as it is possible to observe capacities for several locations.

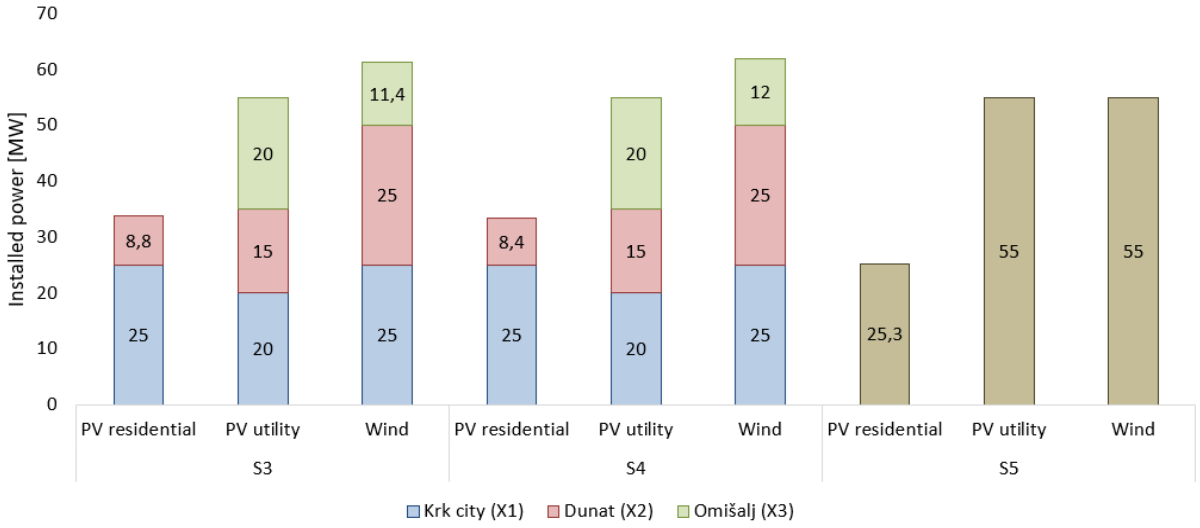

Figure 7. Distribution of installed electricity generation capacities for sensitivity scenarios. In S5, all the technologies were considered to be installed in the same location; thus, they are represented with another color.

Similar results can be observed for the energy storage capacity presented in Figure 8. The differences between S3 and S4 are visible primarily in terms of installed battery storage capacity. Meanwhile, the results of S4 indicated that its installed battery capacity was at 20.2 MWh, while for S3, the battery storage capacity was 24.9 MWh. The reduction of battery capacity is visible for different locations as well. Following the results presented in Figure 7, the difference in spatial modeling between S3 and S5 was significant. Figure 8 shows that the battery storage capacity for S5 was equal to 82.2 MWh, which is 3.3 times higher than the battery capacity for S3. This result indicates the need for spatial distribution modeling in energy planning. Considering S3 as compared to S5, the dispersed energy flows along the entire electrical network allowed a remarkable reduction in the battery storage capacity of the whole energy system. Hydrogen storage also deviated for all three analyzed scenarios, with the highest deviation of 0.5 MWh (between S5 and S3).

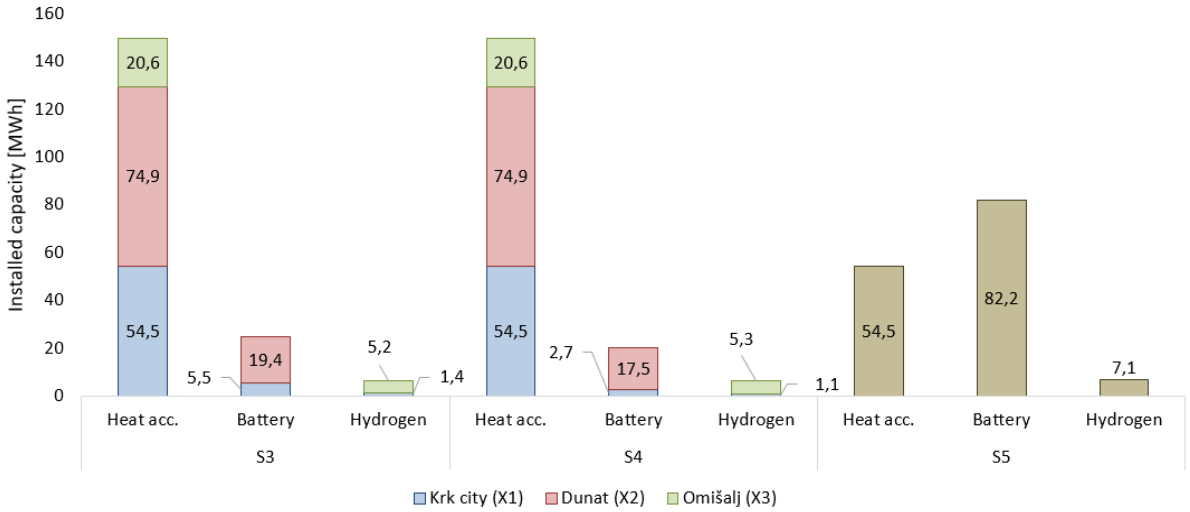

Figure 8. Installed capacities of different storage types in MWh. In S5, all the technologies were considered to be installed in the same location; thus, they are represented with another color.

Capital and operating costs of the five assumed scenarios were then examined. As per the results, similar values were determined for all scenarios except for S5 as can be observed in Figure 9. This result was also in line with the previous findings of the study that showed a significant difference between scenarios that applied different spatial modeling. It should be noted that one of the main reasons for the significant change in S5 is that the scenario does not model the grid connection cost for the potential offshore wind turbine, which is included for S1–S4. In S5, the optimization resulted in the installation of offshore wind turbines instead of onshore ones, as the increased capacity factor has offset the increased capital costs of the technology (Table 7). This result indicated that the cost representation for the spatially distributed scenarios had more realistic value. S3 and S4 also resulted in different total socio-economic costs of the system. The capital system costs of S4 were found to be 0.4% lower than that for S3. Thus, it can be concluded that the half-hourly resolution did not significantly improve the representation of the costs, compared to the hourly temporal resolution.

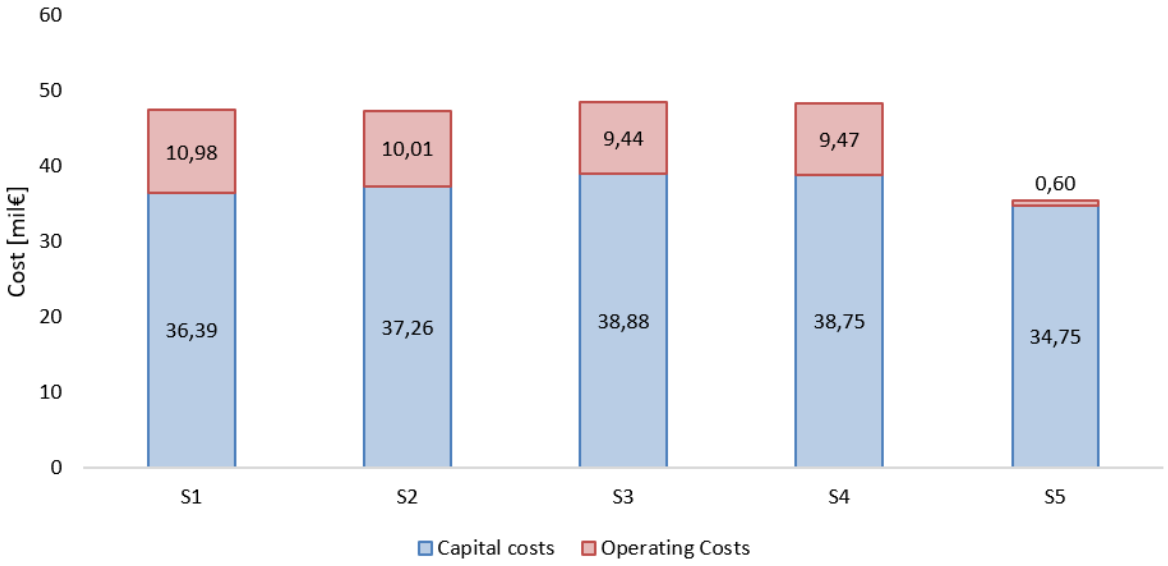

Figure 9. Capital and operating costs for all five scenarios. Internalized costs of CO_2 emissions are included as operating costs.

The following paragraphs focus on the difference in results achieved using different temporal and spatial resolutions. Figure 10 presents the battery storage operation for S3 and S4. Moreover, Figure 10 distinguishes battery storages for two locations—X1 and X2. First, the difference between the different temporal modeling can be observed. This can best be observed for November 4 between midnight and 8:00. The results of the half-hourly scenario (S3) showed the more volatile operation of the battery system storage during this period than for the case of the hourly scenario (S4). On November 5 between 2:00 and 10:00 is also a good example of the benefits of the proposed approach, where charging and discharging of the battery storages occurred only for half-hourly S3. Second, the possibility of observing the operation of different locations for the same scenario allowed more accuracy in energy planning as well. A good example of this is also November 5 where, at 05:00, a sudden 4.72 MWh battery storage system charging occurred at the X2 location. Similar patterns can be observed for the entire period.

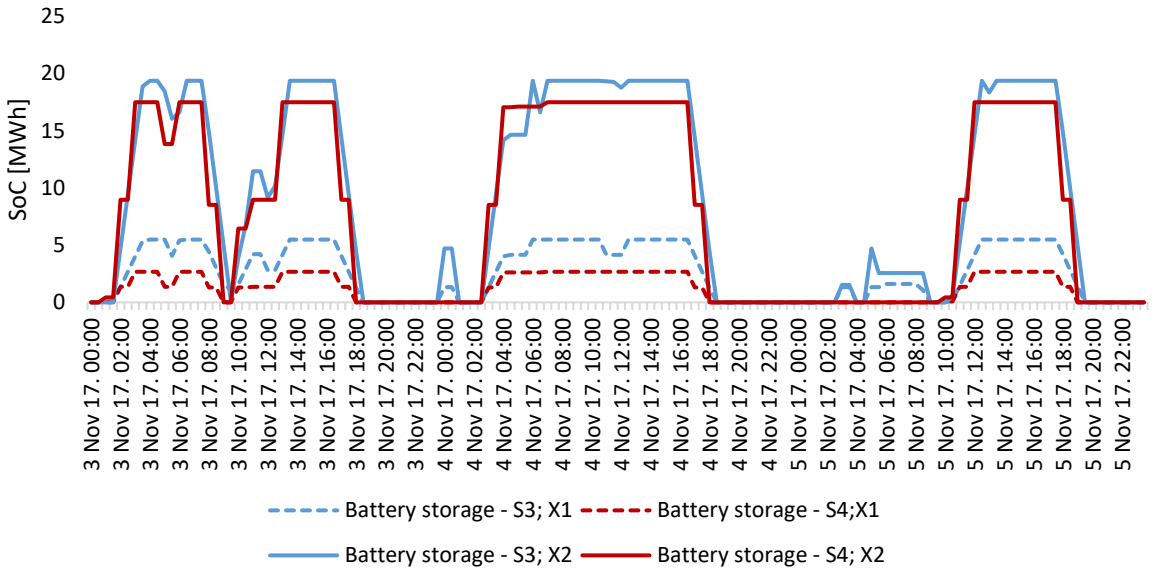

Figure 10. Battery storage operation for S3 and S4 for locations X1 and X2

In Figure 11, the summed battery storage system operation can be observed during May. The results were in line with the findings provided in Figure 10. It can be observed that both scenarios had similar patterns most of the time. However, e differences can be observed, for example, on May 20 in the period 4:30–9:00.

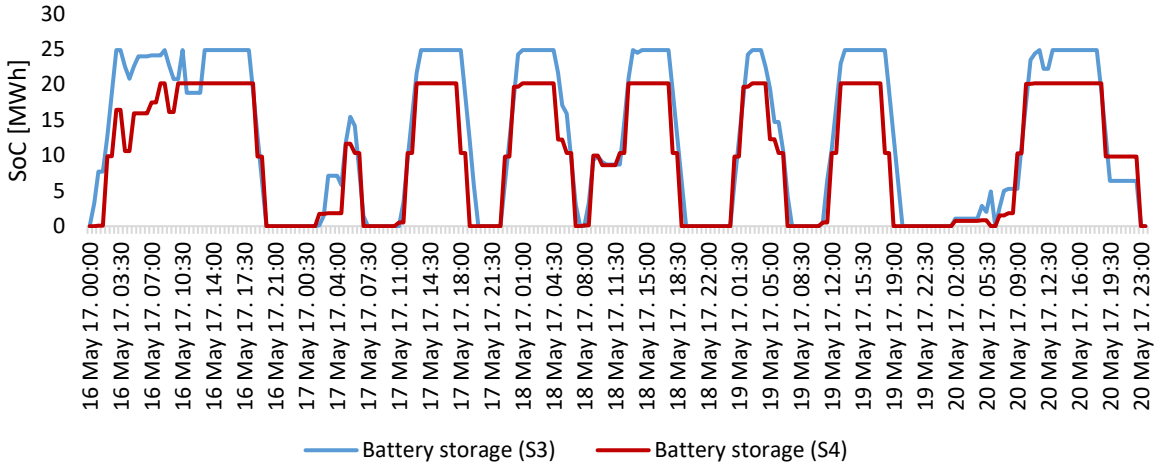

Figure 11. Battery storage operation for the entire Krk Island for S3 and S4

The differences between the two scenarios with different time resolutions were examined for the transport sector as well. Figure 12 presents the end-use power required for the transport sector, namely, the gasoline vehicles and electric vehicles. The end-use power is defined as the power available at wheels of vehicles, meaning that different efficiencies of gasoline and

electric motors cannot be observed in this representation. More detailed representation of the energy system operation was achieved for S3. As shown in Figure 12, the most visible example can be observed on August 5 at 14:00. At this hour, a sudden increase in gasoline demand and a decrease in electricity demand occurred. This change is visible for S3, but not for the hourly scenario S4.

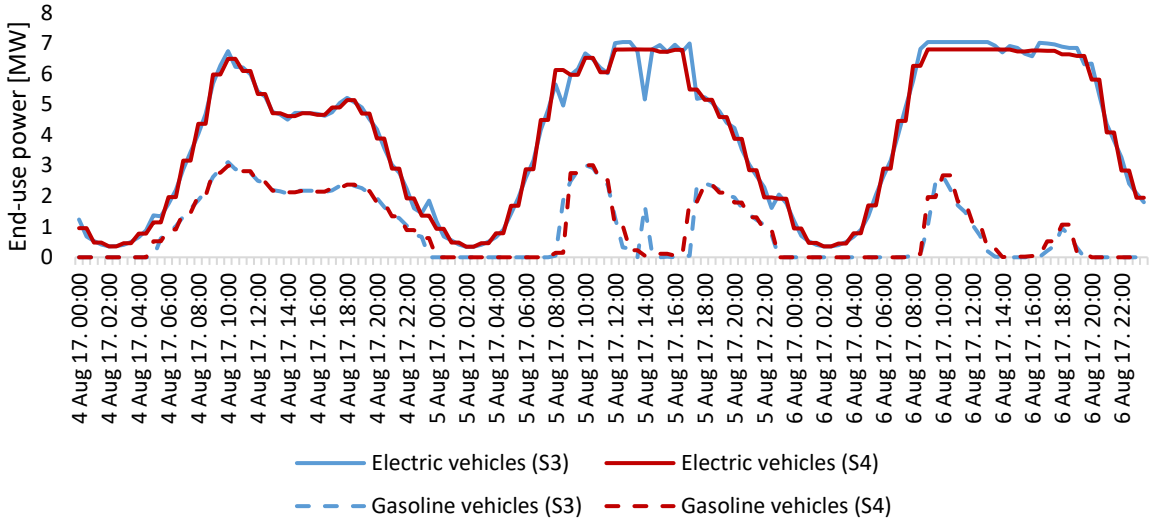

Figure 12. Transport load for S3 and S4 for summer months

The difference in the total SoC of the battery storage system for both scenarios for March is provided in Figure 13. The main difference was in the size of the battery storage systems. The results of S5 with one location modeled indicated several times higher battery storage capacity than the results of S3. Besides the difference in the size of the storages, Figure 13 shows that the trends in the battery system operation are mostly misaligned, especially during charging and discharging periods.

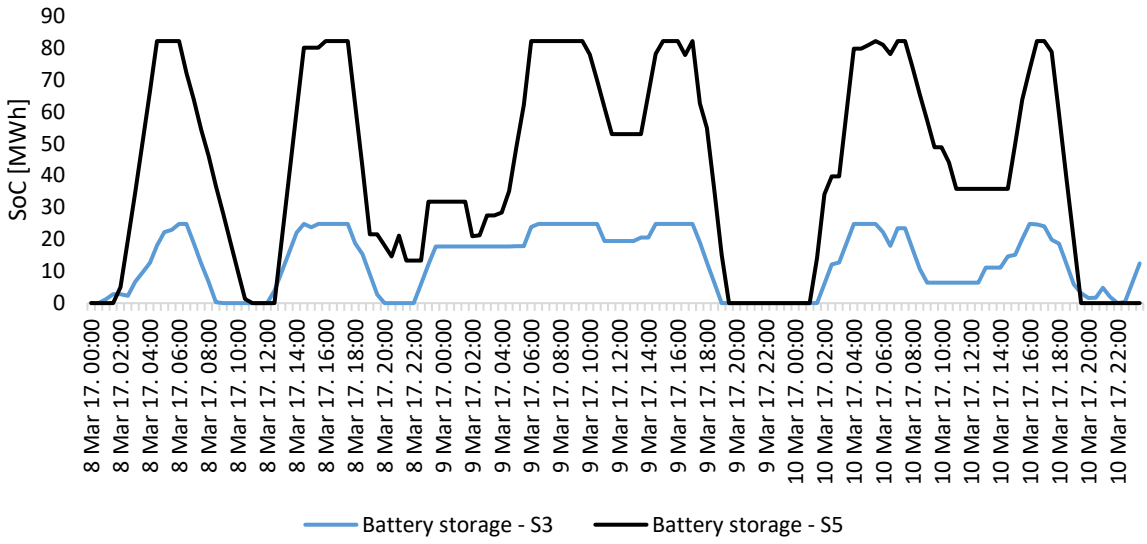

Figure 13. Battery storage operation comparison for S3 and S5

The impact of dispersed spatial modeling was also noted for the transport sector, as shown in Figure 14. The same period was taken as in the scenario analysis of S3 and S4. As per the results, it was determined that S3 and S5 had the same trend for most of the observed period. However, differences occurred for more sudden changes like the one on August 5 at 14:00. Similar to the analysis conducted between S3 and S4, S5 also did not represent this change. The required transport power over time remained approximately the same.

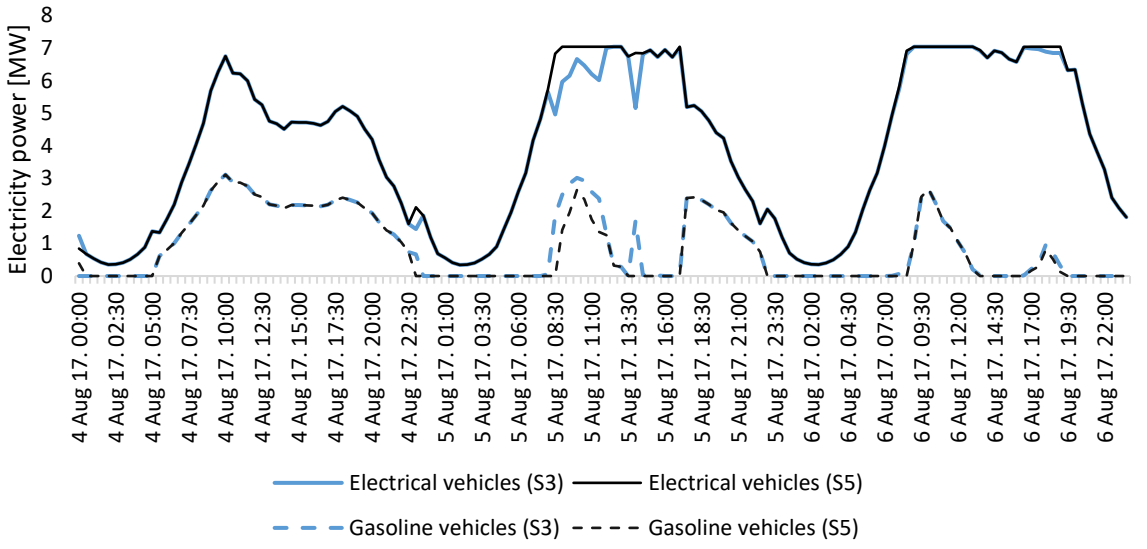

Figure 14. Transport load for S3 and S5 for summer months

4.3.Energy system operation

This chapter presents the key data on the energy system operation of the observed case study. Table 7 presents the overall annual energy production. The results were in line with the previous findings. Slight change in relation to the change in the wind and residential PV production was noted for S1, S2, and S3. The increased level of electrified transport increased the production of these two technologies. Differences are visible for S3 and S4, which could be attributed to the different temporal modeling used for these scenarios. However, the most significant change was noted for S5. The energy system utilized its connection to the mainland grid, resulting in significant export of excess electricity generated on the island. For example, in scenario S3, 16% of the electricity generated by onshore wind, residential, and utility-scale PV were exported. A more detailed figure with exports per locations and technologies can be seen in Appendix B.

Table 7. Annual electricity and thermal energy production

Technology [GWh]	**S1**	**S2**	**S3**	**S4**	**S5**
Residential PV	37.3	42.3	47.3	46.7	36.1
Utility PV	75.4	75.4	75.4	75.4	78.5
Wind **	128.9	132.9	136.6	137.9	265.5
Import	169.9	176	182.5	181.8	100.8
Export	41	40.9	41.6	42.1	96.7
Air HP*	62.5	62.5	62.5	62.5	58.1
BIOboilers*	12.5	12.6	12.5	12.5	16.1

**Thermal energy production*

***In S1–S4, the numbers represent onshore wind production only, while in S5, the number represents offshore and onshore wind production*

Figures 15 and 16 present the operation of the energy system on the Krk Island for winter and summer for S3. The figures provide an insight into the overall operation of the system and the diversity of the installed technologies. It is worth noting that the results have considered the losses in the transmission lines.

Figure 15 presents the operation of the energy system for one day in January. The results showed the dominant influence of wind electricity production for the observed period. Because of this and the lower energy demand during the winter, the export values were determined to be high. As the energy flows were lower during winter months, the corresponding grid losses were also lower. The results showed that the PV generation is less expressed during winter, but

it still provides some of the energy. Grid batteries were mostly charged at night, as a consequence of high wind energy generation in those periods and low electricity prices from the mainland. As the PV generation almost disappeared in this winter day after 13:00, due to overcast, batteries and grid import have helped meeting the demand. This shows the importance of flexibility in the grid such as storage and transmission links. The end of the day was again dominated by wind generation and grid import, while the import increased when the price was low to charge the battery again. During the chosen winter day, the share of PEM electrolyzer consumption in the total final electricity consumption was 1.7%, while the share of final electricity consumed by heat pumps was 39.5%.

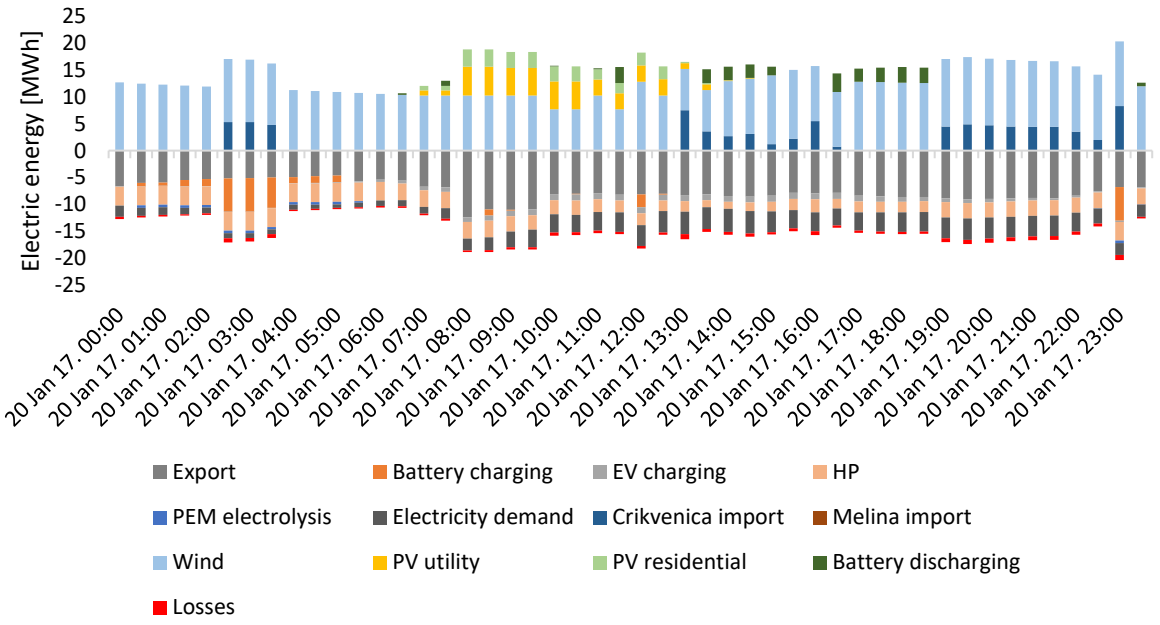

Figure 15. Electricity system operation for two winter days in S3. Export designates the electricity demand of the nearby islands Lošinj (location X4) and Rab (location X5) that have to be supplied through the Krk power grid.

The system operation for summer has been illustrated in Figure 16. With the detailed spatial distribution, it was possible to determine the exact import values from Crikvenica and from Melina, as illustrated in Figure 16. This is expected as the population of Krk can increase up to six times in comparison to the winter period [32]. It was not only the electricity consumption of Krk island that has increased significantly as the same rise in consumption was observed in the nearby islands of Lošinj and Rab. As this consumption needed to be met using the grid of the island of Krk, the total electricity demand in the chosen summer day was 2.5 times higher

than in the chosen winter day. During the night periods, imports from the mainland grid satisfied up to 80% of the consumption. On the other hand, during the day, wind, residential, and utility PV, together with the grid batteries satisfied 100% of the demand in some of the periods (10:00–11:00). It can be observed that much higher grid imports occurred from Crikvenica link (location X7), as this link is connected with the city of Krk consumption point, which has been identified to have the largest electricity demand. The wind production was significantly lower in comparison to the winter period. During the chosen winter day, the share of PEM electrolyzer consumption in the total final electricity consumption was 3%, while the share of final electricity consumed by heat pumps was 15%. The losses in the transmission lines in absolute terms increased as the overall energy flows increased. Batteries were still charged mostly during the night, except for the period from 12:00 to 12:30 as this corresponded with lower mainland grid electricity prices. This representation of the summer day is especially useful to notice wide oscillations between the daily and night operation of the grid. Almost no self-generation during the night is replaced by almost complete self-generation during the day. Thus, it can be seen that for the energy systems of this size, maintaining the link to a larger energy system brings important flexibility to the system, keeping the overall system costs low.

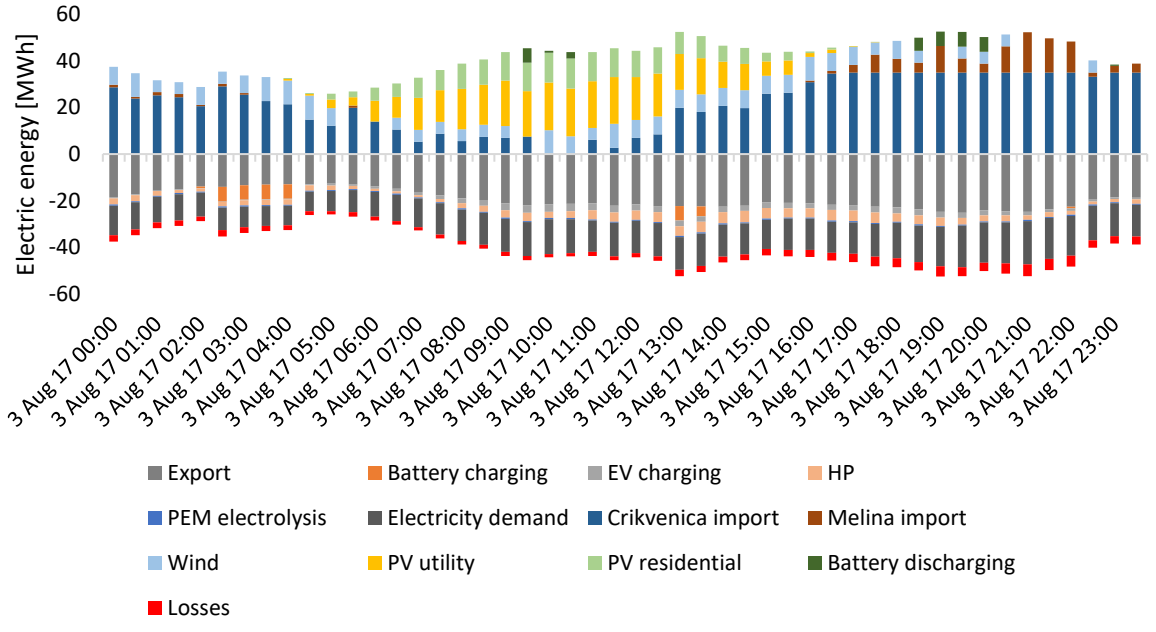

Figure 16. Electricity system operation for two summer days in S3. Export designates the electricity demand of the nearby islands of Lošinj (location X4) and Rab (location X5) that have to be supplied through the Krk power grid.

4.4.Power flow calculation

To assess the impact and evaluate the possibility for the installation of a high amount of variable RES, a power flow calculation has been performed. The calculation was completed for minimum and maximum load and three scenarios. The first scenario is with the state of the currently existing grid at the Krk island, second with the distributed energy resources but without the utility-scale power generations, and, the third scenario, with the utility-scale power generators included at the high voltage bus on the Krk and the Dunat substations. Figures 17 and 18 present the results for the chosen nodes that represent a specific part of the Krk grid. For the case of maximum demand (Figure 17) that occurs during the summer months, it is possible to observe that neither scenario created voltage problems in the grid. Installation of distributed energy resources in the second scenario was determined to have caused an increase in the voltage for all observed nodes, which is already expected. The highest increase of 6.05% was achieved for the Baska 2 node, while the highest voltage value of 1.058 p.u. is recorded for Klimno 1 node. When the utility-scale generations are connected, the highest voltage increase (5.95%) and the highest voltage amount (1.057 p.u.) were recorded for the Dunat substation. As allowed voltage limits range from 0.9 to 1.1 p.u., it can be stated that, for the case of maximum demand, installation of a high amount of variable RES caused the voltage increase but with no threats of violating the voltage limits and without the needed interventions in the electric power grid.

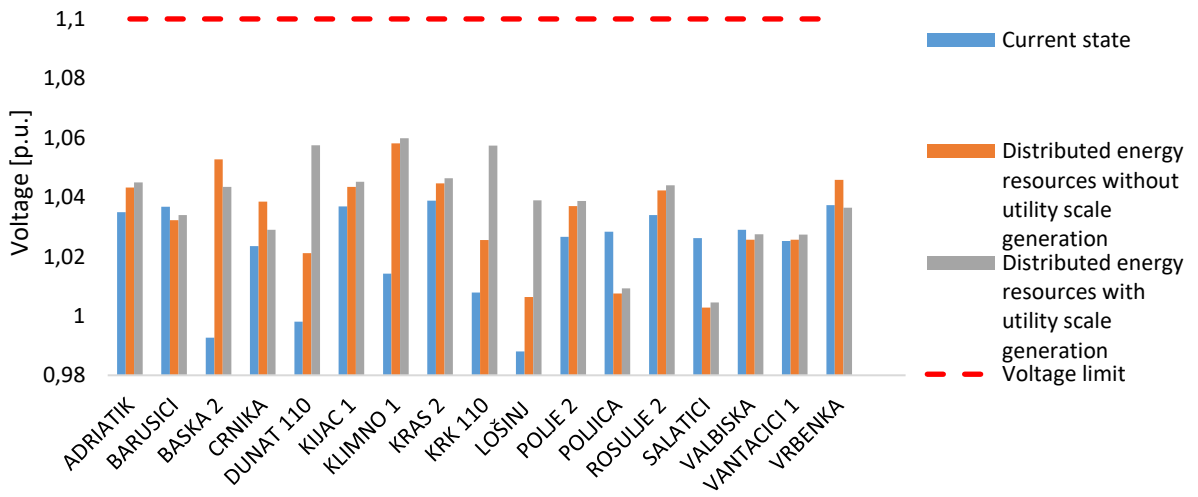

Figure 17. Voltage values for three scenarios at observed nodes for maximum demand case

The results for minimum demand are presented in Figure 18, where it was demonstrated that there was a possible voltage violation on the high voltage buses on Krk, Dunat, and Lošinj substations as well as some distribution transformers located near the high voltage grid (e.g., Poljica and Salatici in Figure 18). This was evident even for the current state of the grid without the connection of the distributed energy resources. The voltage for the current state of the grid was the highest for the Lošinj substation and is equal to 1.128 p.u., but the voltage violations were recorded for Krk (1.125 p.u.) and Dunat (1.125 p.u.). High voltages appeared as a result of low system load during the winter months and the increased reactive power flows in 110 kV grid. Substations Krk and Dunat can be possibly automatically regulated in order to prevent voltage violations in most of the 20 kV grids. However, the voltages were at the higher limit, and some of the nodes violated the limit of 1.1 p.u. (Figure 18). Installation of the distributed energy resources in the medium voltage grid has resulted in voltage increase (the highest increase on Salatica bus of 3.54%, with the voltage value of 1.096 p.u.). The voltages on 110 kV buses also increased by 0.63% at the Dunat substation. When the utility-scale generation was connected as well, the voltage values continued to increase. The voltage at Salatica bus increased by 5.5% and was equal to 1.12 p.u. which is above the limit of 1.1 p.u. Although the medium voltage values remained within the allowed limits for most of the nodes, they were very high and close to the upper limit. It should also be stated that the high voltage values in the medium voltage grid represent the regulation issue at low voltage level as the distribution transformers 20/0.42 kV are required to regulate low voltage values, which may only impose an issue.

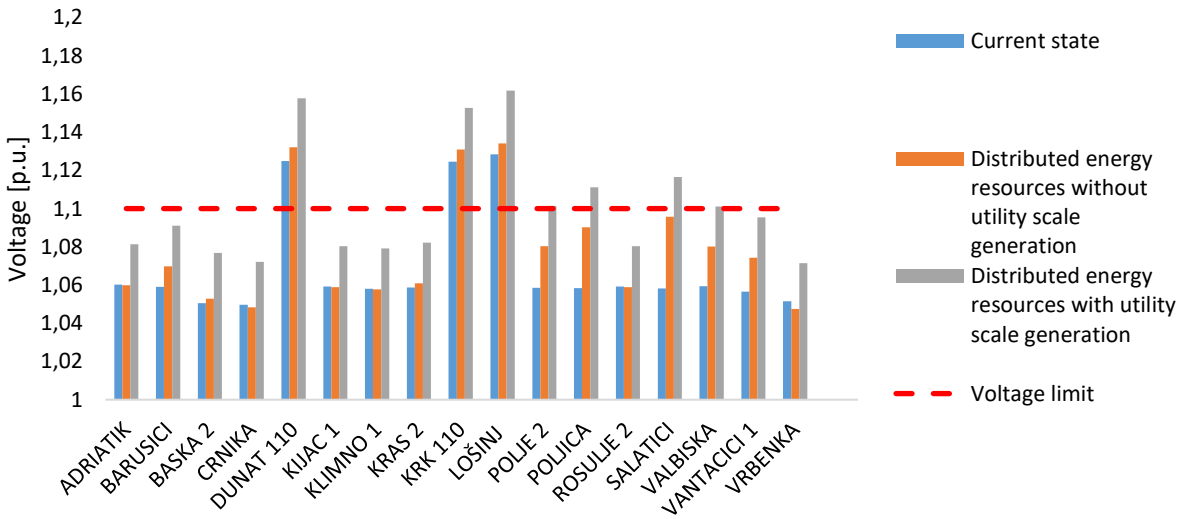

Figure 18. Voltage values for three scenarios at observed nodes for minimum demand case

Although voltage increase is evident for all cases during minimum load, the issue could be resolved by the installation of a 300 Mvar coil in high voltage substation Melina [59]. Installation of this coil would significantly reduce reactive power flows during periods of lower load, thus reducing voltage to its nominal limits. Such installation would also enable installation of proposed energy planning scenarios in this study as well.

4.5.Socio-economic analysis

Using the explained job creation method, the proposed energy scenarios would result in 2435 created job-years on the global scale as well as 45 permanent local jobs. Since these are high-profile green jobs, the proposed energy planning scenarios would have a significant positive impact on the economy that is currently heavily dependent on seasonal tourism. For example, when considering the Krk island population, this would mean that 2.3 permanent local jobs for 1000 residents would be created as a result of decarbonization of the island energy system. It should also be noted that these numbers are obtained without consideration of transport electrification and energy storage systems as there is still no unique approach on how to calculate created jobs as a result of the installation of these technologies.

5. Discussion

The main findings of this paper are related to both detailed spatial and temporal modeling of the capacity expansion problem of the island energy system. This research was enhanced by modeling both the transmission and distribution systems of the island and the validation of the capacity expansion modeling results via power flow analysis.

This study showed that the detailed spatial resolution is more important than the very detailed temporal resolution. However, one has to take into account that hourly resolution is already considered a detailed one for the capacity expansion problems. This study has further showed that a more detailed spatial representation has a significant impact on the calculation of the total system costs and optimal technology mix, it does not underestimate the import needs for electricity from the mainland grid, and it does not overestimate the potential for exporting the electricity to the mainland grid. Furthermore, a coarser spatial representation significantly underestimates the capacity needs for storage technologies that are needed in the energy system.

To the best of our knowledge, the most detailed research on temporal and spatial trade-offs so far has been carried out in [60]. The authors concluded that the most trade-offs between temporal and spatial resolution have yielded up to 15% of cost differences. Concerning the spatial resolution, the authors showed that the uniform buildout case resulted in a 10% reduction in cost compared to the site-by-site buildout case. Focusing on temporal resolution, the authors showed that the total cost is significantly lower with a coarser temporal resolution. In this paper, a fine (hourly) and a very fine (half-hourly) temporal resolution yielded a rather small cost difference, i.e., 0.4%. However, a difference between a detailed and coarse spatial representation yielded a difference in costs of 26.7%, which is significantly higher than that in [60].

Detailed transmission and distribution representation realistically captured possible congestions and resulted in a realistic representation of optimal capacities of distributed energy systems. With the application of the power flow analysis, it was possible to validate the results from the detailed spatiotemporal model. A detailed flow analysis has showed that the voltage levels would violate the allowed values in the scenario with the largest share of grid loading and the variable renewable energy generation (S3), which would result in a distribution system operator's ban on the development before the necessary actions would be taken into account. For this specific case study, an installation of 300 Mvar coils would solve these grid issues. This shows that the usual capacity expansion planning models with a high share of variable renewable energy generation, and a higher share of electric transport, are potentially underestimating grid constraints that cannot be simply evaluated just by modeling simple grid capacity constraints. The soft-linking of PLEXOS and TIMES model was presented in [61]. However, the PLEXOS model was run as a unit commitment and the power flow calculation was not performed. The study in this paper used a more detailed Calliope and power flow model with focus on the feasibility of the problem and the detailed spatiotemporal modeling which was not the case in [61]. An approach to soft-link capacity expansion models and more detailed operational once has been recently proposed for a specific sector, such as district heating [62]. However, this paper expands the same approach to the integrated energy system capacity expansion model, which takes into account a number of different energy sectors including heating and cooling system. This approach enables to analyze the interconnection between different energy vectors in detail which was not the case in [62]. This study [63] analyzed a similar case study with lower electricity consumption and suggested the energy planning system with 30 MW of installed PV and 22 MW of installed wind. The results from the power flow

analysis conducted in this paper indicated that a similar analysis should be constructed in the study [63] in order to assess the implementation possibilities for the proposed scenario.

This paper has also introduced simple job analysis potential modeling as part of the socio-economic analysis. This is the consequence of the rising resistance of the local communities toward installing large amounts of distributed energy systems in their vicinity [64]. If a successfully high local job creation potential can be achieved, it is expected that the local resistance toward the implementation of the renewable energy projects will subside. On top of the local job creation potential, an additional economic benefit could be gained if local residents would be involved as stakeholders in the investments in energy sector facilities. Such inclusion would have social benefits as well, as residents would become more involved in the energy sector, thus leading to the creation of an energy community. Example of such successful small-scale project is given in [65] where citizens were involved in a crowdfunding campaign for the financing of a rooftop solar power plant. In another initiative [66] on the island in Denmark, 650 local citizens became the owners of 6 wind turbines.

Although the methods were applied for a specific case, the methods applied in this case study did not have many case-specific site constraints, creating a higher potential to apply the developed methods to other case studies. It is expected that the developed methods are applicable to many different regions, especially islands connected to the main grid. Most especially, islands in the Mediterranean and tropical belt have a high potential for variable RES. However, the methods developed in this paper showed that islands' power grids could be severely impacted by the large renewable energy capacities and, thus, should follow a more detailed capacity expansion and power flow grid analysis. Moreover, the presented method is especially beneficial for the areas with weaker grids where the integration of RES may be more difficult. It is estimated that there are 11,000 inhabited islands in the world [67], providing many opportunities to test the developed method.

There are several limitations to this study. The goal of the capacity expansion model was on minimizing the total socio-economic costs of the system. Although those are the true costs imposed on the society, the business-economic case for specific investments can significantly vary depending on the risks, regulations, and laws that influence investment decisions. Moreover, an approach of the first-mover into a rapid increase in the share of variable renewable energy capacity was assumed in this paper. It was shown that the island can benefit also from exporting access to the energy generated (Appendix B). If the whole country would undertake a similar transition, there would be fewer opportunities to export excess electricity generated

for good prices, as well as fewer opportunities to use its batteries for price arbitrage. Furthermore, on-demand charging strategy for vehicles was adopted in all the scenarios. Although left outside of the scope of this study, considerations on smart charging and vehicle-to-grid options could significantly influence grid conditions. It is recommended that for future studies, the same methods developed in this paper be expanded to account for more detailed representation of the transport sector strategies.

Finally, this paper was developed fully adopting the open-access goals, using a fully open-source modeling tool, as well as publishing all the data, coding scripts, and results via a public site [42], documenting the steps needed to rerun the model. This will allow for better and faster exchange of ideas within the scientific community, resulting in more rapid improvements in the methods developed in this paper.

6. Conclusions

This paper presented a novel approach for energy planning of interconnected islands. As per our findings, it was determined that taking spatial distribution and the half-hourly distribution into account has resulted in more accurate results in comparison with the previous similar studies that have analyzed the energy systems on the islands. The main conclusions of the study were as follows:

- The results indicated that the total cost for the spatially distributed scenario was 26.7% higher than the scenario with the technologies aggregated in one location. Additionally, the results showed that 3.3 times higher battery capacity was required for the coarser scenario, which leads to the conclusion that detailed spatial modeling significantly improves the energy planning process.
- The comparison between the half-hourly and hourly time resolution modeling resulted in a 0.2% lower total cost for the half-hourly scenario and an 18.9% higher battery storage capacity for the half-hourly scenario. It is possible to conclude that the half-hourly time resolution also improves the energy planning process; however, the improvement is less expressed than for the case of spatial modeling application.
- The presented approach validated the results of the energy system analysis by conducting the power system analysis as the latter provided insights into the voltage and power flows of the analyzed island system. These results showed that several nodes had voltage values higher than 1.1 p.u. and did not satisfy the grid code regulations, which

indicates the need for the power system analysis of the energy planning scenarios for the assessment of the implementation possibilities.

Future research should be geared toward the inclusion of other sectors, such as the water sector, in the model in order to quantify the flexibility of the proposed energy planning scenarios. The use of the ICT for smart charging and the usage of batteries for ancillary service management are examples of the features that will need to be considered in the future models. The soft-linking between the energy planning model and the power flow analysis model will also be further investigated in order to improve the approximation of the grid constraints in the energy planning models. This would result in higher application potential of the energy planning scenarios.

Appendix A

Newton-Raphson method is an iterative method used for solving power flow problem in the electric power grid and it is used in this study. Appendix A provides insight into how the method is defined.

Let voltage and admittance matrix Y elements be defined as:

$$\overline{V_i} = V_i \angle \delta_i, \overline{V_j} = V_j \angle \delta_j \quad \text{(A.1)}$$

$$\overline{Y_{ij}} = Y_{ij} \angle \theta_{ij} \quad \text{(A.2)}$$

Where i and j represent the nodes in the system, V is the voltage amount at a node, δ is the voltage angle, Y is the value of admittance matrix element and θ is the admittance matrix element angle. Active (P) and reactive power (Q) at power system nodes can be expressed as:

$$P_i = \sum_{j=1}^{n} V_i Y_{ij} V_j \cos(\delta_i - \theta_{ij} - \delta_j) \quad \text{(A.3)}$$

$$Q_i = \sum_{j=1}^{n} V_i Y_{ij} V_j \sin(\delta_i - \theta_{ij} - \delta_j) \quad \text{(A.4)}$$

The fundamental matrix equation for the Newton-Raphson procedure can be expressed as (A.5):

$$\begin{bmatrix} \Delta P \\ \Delta Q \end{bmatrix} = \begin{bmatrix} J_1 & J_2 \\ J_3 & J_4 \end{bmatrix} \cdot \begin{bmatrix} \Delta \delta \\ \Delta V \end{bmatrix} \quad \text{(A.5)}$$

Where J_1,…, J_4 represent sub-matrix of the Jacobian matrix and their elements are calculated by deriving equations (A.3) and (A.4). From these expressions it is possible to obtain full expression of (A.5) equation:

$$\begin{bmatrix} \Delta P_1 \\ \vdots \\ \Delta P_{n-1} \\ \Delta Q_1 \\ \vdots \\ \Delta Q_{n-1-g} \end{bmatrix} = \begin{bmatrix} \frac{\partial P_1}{\partial \delta_1} & \cdots & \frac{\partial P_1}{\partial \delta_{n-1}} & \frac{\partial P_1}{\partial V_1} & \cdots & \frac{\partial P_1}{\partial V_{n-1-g}} \\ \vdots & \ddots & \vdots & \vdots & \ddots & \vdots \\ \frac{\partial P_{n-1}}{\partial \delta_1} & \cdots & \frac{\partial P_{n-1}}{\partial \delta_{n-1}} & \frac{\partial P_{n-1}}{\partial V_1} & \cdots & \frac{\partial P_{n-1}}{\partial V_{n-1-g}} \\ \frac{\partial Q_1}{\partial \delta_1} & \cdots & \frac{\partial Q_1}{\partial \delta_{n-1}} & \frac{\partial Q_1}{\partial V_1} & \cdots & \frac{\partial Q_1}{\partial V_{n-1-g}} \\ \vdots & \ddots & \vdots & \vdots & \ddots & \vdots \\ \frac{\partial Q_{n-1-g}}{\partial \delta_1} & \cdots & \frac{\partial Q_{n-1-g}}{\partial \delta_{n-1}} & \frac{\partial Q_{n-1-g}}{\partial V_1} & \cdots & \frac{\partial Q_{n-1-g}}{\partial V_{n-1-g}} \end{bmatrix} \cdot \begin{bmatrix} \Delta \delta_1 \\ \vdots \\ \Delta \delta_{n-1} \\ \Delta V_1 \\ \vdots \\ \Delta V_{n-1-g} \end{bmatrix} \quad \text{(A.6)}$$

Where g is the number of generating nodes that can control voltage at the desired value. Therefore, in these nodes, it is not necessary to calculate voltage, but only reactive power according to (A.4) and check if the reactive power is within the allowed limits $Q \in [Q_{min}, Q_{max}]$. If the reactive power is not within these limits, the observed node becomes PQ node (where active and reactive power is known) with reactive power at its limit (Q_{min} or Q_{max}).

Since voltage amount change to active power change can be neglected and voltage angle change to reactive power change can be neglected as well, it is possible to apply some relaxations and assign zero value to elements of sub-matrix J_2 and J_3. For this case, it is possible to separately observe equations of active power change to voltage angle change and reactive power change to voltage amount change. Equation (A.5) can then be written as (A.7):

$$\begin{bmatrix} \Delta P \\ \Delta Q \end{bmatrix} = \begin{bmatrix} J_1 & 0 \\ 0 & J_4 \end{bmatrix} \cdot \begin{bmatrix} \Delta \delta \\ \Delta V \end{bmatrix} \quad \text{(A.5)}$$

By solving the system of equations stated in (A.5) with iterative Newton-Raphson procedure it is possible to calculate voltages and reactive and active power flow in the electric power grid. The difference between power production and demand is covered from the slack node that is connected to an external grid. Simplified Newton-Raphson procedure is described in a diagram presented in Figure A.1.

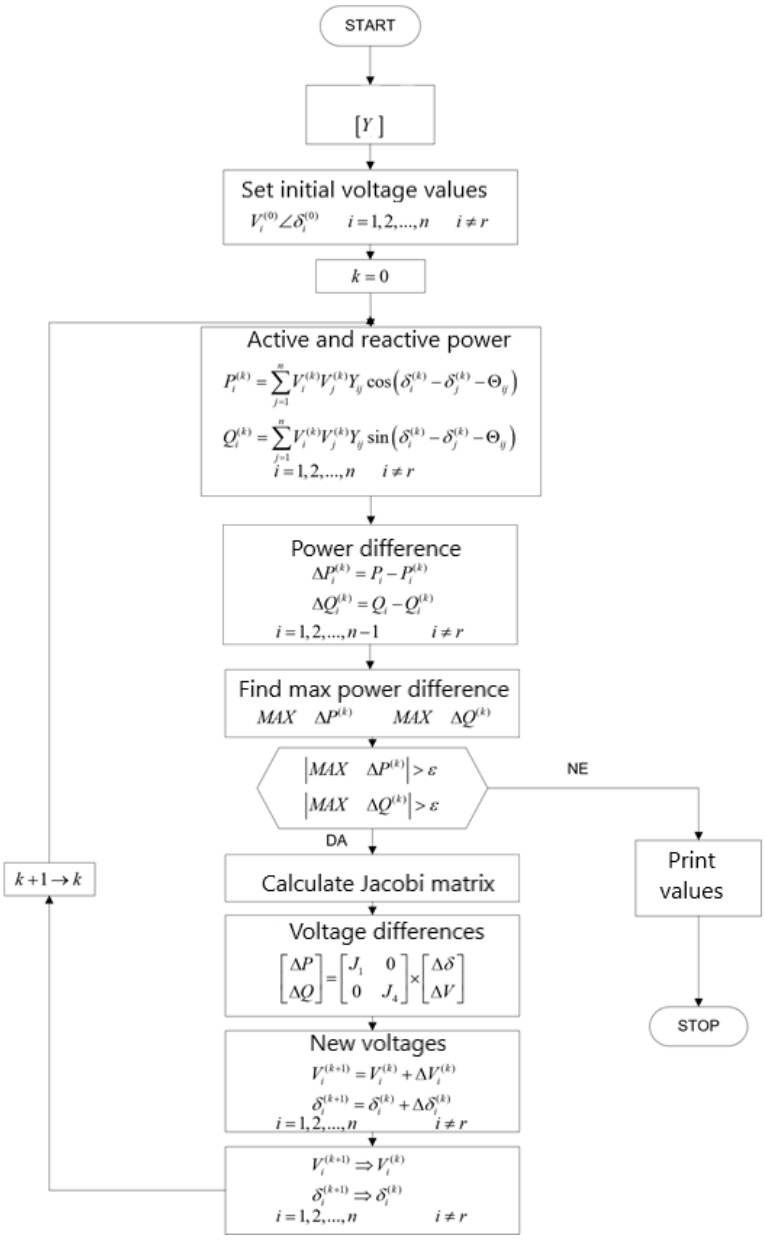

Figure A.1. Diagram for power flow calculation using Newton-Raphson

Appendix B

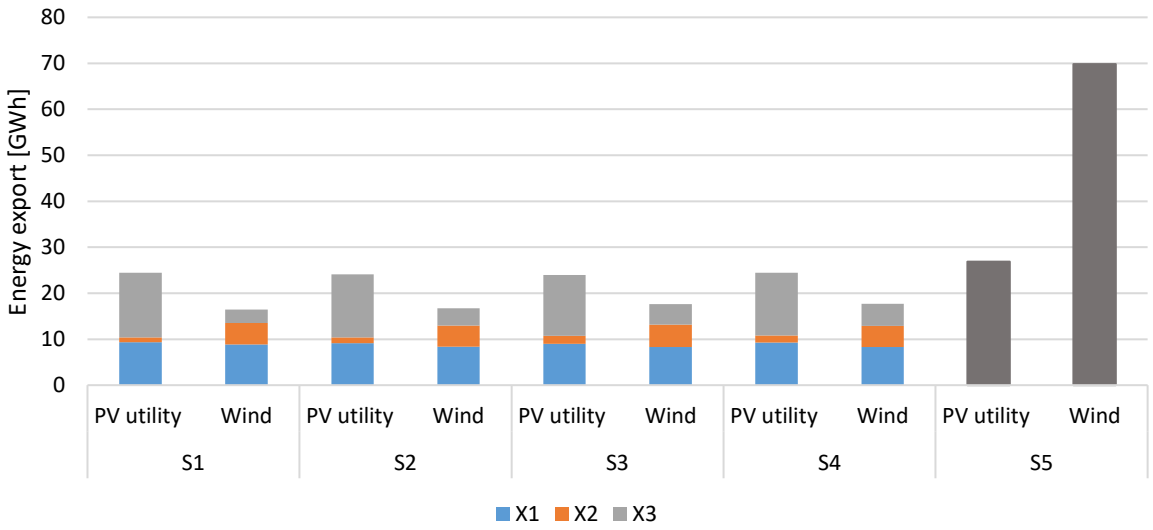

Figure B.1. Energy export values for analysed scenarios and different locations – the scenario S5 is presented with different colour as only one location is considered for S5

Acknowledgement

This work has been supported by the Young Researchers' Career Development Programme (DOK-01-2018) of Croatian Science Foundation which is financed by European Union from European Social Fund and Horizon 2020 project INSULAE - Maximizing the impact of innovative energy approaches in the EU islands (Grant number ID: 824433). Moreover, this project was also funded by CITIES project nr. DSF1305-00027B, funded by the Danish Innovationsfonden. The stated support is gratefully acknowledged. The link with detailed energy system model is provided at https://github.com/CROdominik/Krk_Calliope_energy_model.

References

[1] Hauer ME, Fussell E, Mueller V, Burkett M, Call M, Abel K, et al. Sea-level rise and human migration. Nat Rev Earth Environ 2020;1. https://doi.org/10.1038/s43017-019-

0002-9.

[2] DAFNI. Smart Island Initiative. Netw Sustain Greek Islands 2017.

[3] European Commission. Clean Energy for EU Islands launch. Eur Comm Energy News 2017.

[4] Chandran CV, Basu M, Sunderland K, Pukhrem S, Catalão JPS. Application of demand response to improve voltage regulation with high DG penetration. Electr Power Syst Res 2020;189. https://doi.org/10.1016/j.epsr.2020.106722.

[5] Segurado R, Krajačić G, Duić N, Alves L. Increasing the penetration of renewable energy resources in S. Vicente, Cape Verde. Appl Energy 2011. https://doi.org/10.1016/j.apenergy.2010.07.005.

[6] Segurado R, Costa M, Duić N, Carvalho MG. Integrated analysis of energy and water supply in islands. Case study of S. Vicente, Cape Verde. Energy 2014. https://doi.org/10.1016/j.energy.2015.02.013.

[7] Child M, Nordling A, Breyer C. Scenarios for a sustainable energy system in the Åland Islands in 2030. Energy Convers Manag 2017. https://doi.org/10.1016/j.enconman.2017.01.039.

[8] Curto D, FRANZITTA V, Trapanese M, Cirrincione M. A Preliminary Energy Assessment to Improve the Energy Sustainability in the Small Islands of the Mediterranean Sea. J Sustain Dev Energy, Water Environ Syst 2020; https://doi.org/10.13044/j.sdewes.d7.0314.

[9] Ocon JD, Bertheau P. Energy transition from diesel-based to solar photovoltaics-battery-diesel hybrid system-based island grids in the Philippines – Techno-economic potential and policy implication on missionary electrification. J Sustain Dev Energy, Water Environ Syst 2019;7. https://doi.org/10.13044/j.sdewes.d6.0230.

[10] Meschede H, Child M, Breyer C. Assessment of sustainable energy system configuration for a small Canary island in 2030. Energy Convers Manag 2018. https://doi.org/10.1016/j.enconman.2018.03.061.

[11] Curto D, Franzitta V, Viola A, Cirrincione M, Mohammadi A, Kumar A. A renewable energy mix to supply small islands. A comparative study applied to Balearic Islands and Fiji. J Clean Prod 2019;241. https://doi.org/10.1016/j.jclepro.2019.118356.

[12] Holjevac N, Capuder T, Zhang N, Kuzle I, Kang C. Corrective receding horizon scheduling of flexible distributed multi-energy microgrids. Appl Energy 2017. https://doi.org/10.1016/j.apenergy.2017.06.045.

[13] Gils HC, Simon S. Carbon neutral archipelago – 100% renewable energy supply for the Canary Islands. Appl Energy 2017. https://doi.org/10.1016/j.apenergy.2016.12.023.

[14] Pfeifer A, Dobravec V, Pavlinek L, Krajačić G, Duić N. Integration of renewable energy and demand response technologies in interconnected energy systems. Energy 2018. https://doi.org/10.1016/j.energy.2018.07.134.

[15] Fichera A, Pluchino A, Volpe R. From self-consumption to decentralized distribution among prosumers: A model including technological, operational and spatial issues. Energy Convers Manag 2020;217. https://doi.org/10.1016/j.enconman.2020.112932.

[16] Fichera A, Frasca M, Palermo V, Volpe R. An optimization tool for the assessment of urban energy scenarios. Energy 2018;156. https://doi.org/10.1016/j.energy.2018.05.114.

[17] Pavičević M, Mangipinto A, Nijs W, Lombardi F, Kavvadias K, Jiménez Navarro JP, et al. The potential of sector coupling in future European energy systems: Soft linking between the Dispa-SET and JRC-EU-TIMES models. Appl Energy 2020;267. https://doi.org/10.1016/j.apenergy.2020.115100.

[18] Blanco H, Gómez Vilchez JJ, Nijs W, Thiel C, Faaij A. Soft-linking of a behavioral model for transport with energy system cost optimization applied to hydrogen in EU. Renew Sustain Energy Rev 2019;115. https://doi.org/10.1016/j.rser.2019.109349.

[19] Dominkovic DF, Stark G, Hodge BM, Pedersen AS. Integrated energy planning with a high share of variable renewable energy sources for a Caribbean Island. Energies 2018. https://doi.org/10.3390/en11092193.

[20] Milano F. Power system modelling and scripting. Power Syst 2010. https://doi.org/10.1007/978-3-642-13669-6.

[21] Imen L, Djamel L, Hassiba S, Abdellah D, Selwa F. Optimal power flow study using conventional and neural networks methods. 2015 Int. Conf. Renew. Energy Res. Appl. ICRERA 2015, 2015. https://doi.org/10.1109/ICRERA.2015.7418642.

[22] Weckesser T, Dominković DF, Blomgren EMV, Schledorn A, Madsen H. Renewable Energy Communities: Optimal sizing and distribution grid impact of photo-voltaics and

battery storage. Appl Energy 2021;301:117408. https://doi.org/10.1016/J.APENERGY.2021.117408.

[23] Pfenninger S, Pickering B. Calliope: a multi-scale energy systems modelling framework. J Open Source Softw 2018;3. https://doi.org/10.21105/joss.00825.

[24] Hilpert S, Kaldemeyer C, Krien U, Günther S, Wingenbach C, Plessmann G. The Open Energy Modelling Framework (oemof) - A new approach to facilitate open science in energy system modelling. Energy Strateg Rev 2018;22:16–25. https://doi.org/10.1016/j.esr.2018.07.001.

[25] Pfenninger S. Calliope - case studies 2019. https://www.callio.pe/model-gallery/ (accessed 23rd September 2019).

[26] Dominković DF, Bačeković I, Pedersen AS, Krajačić G. The future of transportation in sustainable energy systems: Opportunities and barriers in a clean energy transition. Renew Sustain Energy Rev 2018. https://doi.org/10.1016/j.rser.2017.06.117.

[27] Calliope. Calliope documentation: Mathematical formulation, https://calliope.readthedocs.io/en/stable/user/ref_formulation.html (accessed 19th August 2021) n.d.

[28] Dominković DF, Bačeković I, Sveinbjörnsson D, Pedersen AS, Krajačić G. On the way towards smart energy supply in cities: The impact of interconnecting geographically distributed district heating grids on the energy system. Energy 2017;137:941–60. https://doi.org/10.1016/j.energy.2017.02.162.

[29] Ferroukhi R, Khalid A, Lopez-Peña A, Renner M. "Renewable Energy and Jobs: Annual Review 2014." Int Renew Energy Agency 2014.

[30] Busarello, Cott, Partner Inc., ABB Utilities Gmbh. NEPLAN Users' guide Electrical, 2015; Version 5.

[31] Bauer N, Edenhofer O, Kypreos S. Linking energy system and macroeconomic growth models. Comput Manag Sci 2008;5. https://doi.org/10.1007/s10287-007-0042-3.

[32] Republic of Croatia – Central Bureau of Statistics. Census of Population, Households and Dwellings 2011; (in Croatian)

[33] Dominković DF, Dobravec V, Jiang Y, Nielsen PS, Krajačić G. Modelling smart energy

systems in tropical regions. Energy 2018;155:592–609. https://doi.org/10.1016/j.energy.2018.05.007.

[34] https://www.google.com/maps n.d. (accesed 10th November 2020)

[35] BEIS, UK Government, The Clean Growth Strategy: Leading the way to a low carbon future, 2017.

[36] https://www.amsterdam.nl/en/policy/sustainability/policy-phasing-out/ (accessed 7th February 2021) n.d.

[37] rp5 weather archive. rp5.ru weather forecast. Online Arch 2020.

[38] European Commission. EU Science Hub: pvgis. Online Database 2020.

[39] Dominkovic DF, Mimica M. Krk (Croatia) Calliope Energy model - https://github.com/CROdominik/Krk_Calliope_energy_model. Github 2020. (accessed 19th August 2021)

[40] Rosenthal P, Sišul Jurković S, Josipović S, Goreta D. Zero emission interdisciplinary strategy for sustainable development of Krk island. 2012.

[41] Čotar A, Hunjak S, Jardas D. Sustainable energy action plan of Krk city. 2016.

[42] Radulović D, Klanac A. Sustainable energy action plan of Vrbnik municipality. 2015. (in Croatian)

[43] Variola D. Electric power system modeling of Krk island. Univerity of Rijeka, 2017 (in Croatian)

[44] Božić M, Kopić D, Mihoci F, Marold N, Gršetić J. Traffic count report for Republic of Croatia 2017. 2018. (in Croatian)

[45] DHMZ. Krk solar irradiation measurements. 2016.

[46] http://rp5.ru/metar.php?metar=LDRI&lang=en (accessed 9th September 2020) n.d.

[47] Danish Energy Agency, Energinet. Technology data - Energy storage. 2018.

[48] Danish Energy Agency, Energinet. Technology data - Energy plants for Electricity and District heating generation. 2016.

[49] IRENA. Renewable Power Generation Costs in 2017. 2018.

[50] Danish Energy Agency, Energinet. Technology data - Renewable fuels. 2017.

[51] Danish Energy Agency, Energinet. Technology data for heating installations. 2016.

[52] Danish Energy Agency. Technology datasheet - Industrial process heat and cc. 2020.

[53] Danish Energy Agency, Energinet. Technology data - Energy transport. 2017.

[54] www.cropex.hr (accessed 11th February 2020) n.d.

[55] EMBER. EUA Price. Database 2020.

[56] Lewis M. Carbon Clampdown - Closing the Gap to a Paris-compliant EU-ETS 2018;1–76.

[57] Cerovečki T, Cvitanović M, Damjanović F, Ivković R, Majcen J, Širić I. Optimal technical connection of PV plant on distribution grid 2019. (in Croatian)

[58] Dominković DF, Bačeković I, Ćosić B, Krajačić G, Pukšec T, Duić N, et al. Zero carbon energy system of South East Europe in 2050. Appl Energy 2016;184. https://doi.org/10.1016/j.apenergy.2016.03.046.

[59] https://www.sincrogrid.eu/en (accessed 11th May 2020) n.d.

[60] Frew BA, Jacobson MZ. Temporal and spatial tradeoffs in power system modeling with assumptions about storage: An application of the POWER model. Energy 2016;117:198–213. https://doi.org/10.1016/j.energy.2016.10.074.

[61] Deane JP, Chiodi A, Gargiulo M, Ó Gallachóir BP. Soft-linking of a power systems model to an energy systems model. Energy 2012;42. https://doi.org/10.1016/j.energy.2012.03.052.

[62] Dominković DF, Junker RG, Lindberg KB, Madsen H. Implementing flexibility into energy planning models: Soft-linking of a high-level energy planning model and a short-term operational model. Appl Energy 2020;260. https://doi.org/10.1016/j.apenergy.2019.114292.

[63] Dorotić H, Doračić B, Dobravec V, Pukšec T, Krajačić G, Duić N. Integration of transport and energy sectors in island communities with 100% intermittent renewable energy sources. Renew Sustain Energy Rev 2019. https://doi.org/10.1016/j.rser.2018.09.033.

[64] McKenna R, Ryberg DS, Staffell I, Hahmann AN, Schmidt J, Heinrichs H, et al. On the socio-technical potential for onshore wind in Europe: A response to Enevoldsen et al. (2019), Energy Policy, 132, 1092-1100. Energy Policy 2020;145:1–6. https://doi.org/10.1016/j.enpol.2020.111693.

[65] https://www.zez.coop/ulaganja/ (accessed 7th September 2020) n.d.

[66] https://www.euislands.eu/aero-finance (accessed 24th November 2020) n.d.

[67] Meschede H, Holzapfel P, Kadelbach F, Hesselbach J. Classification of global island regarding the opportunity of using RES. Appl Energy 2016. https://doi.org/10.1016/j.apenergy.2016.05.018.